Article

Cell Reports

In Vivo Suppression of HIV Rebound by Didehydro-Cortistatin A, a "Block-and-Lock" Strategy for HIV-1 Treatment

Graphical Abstract

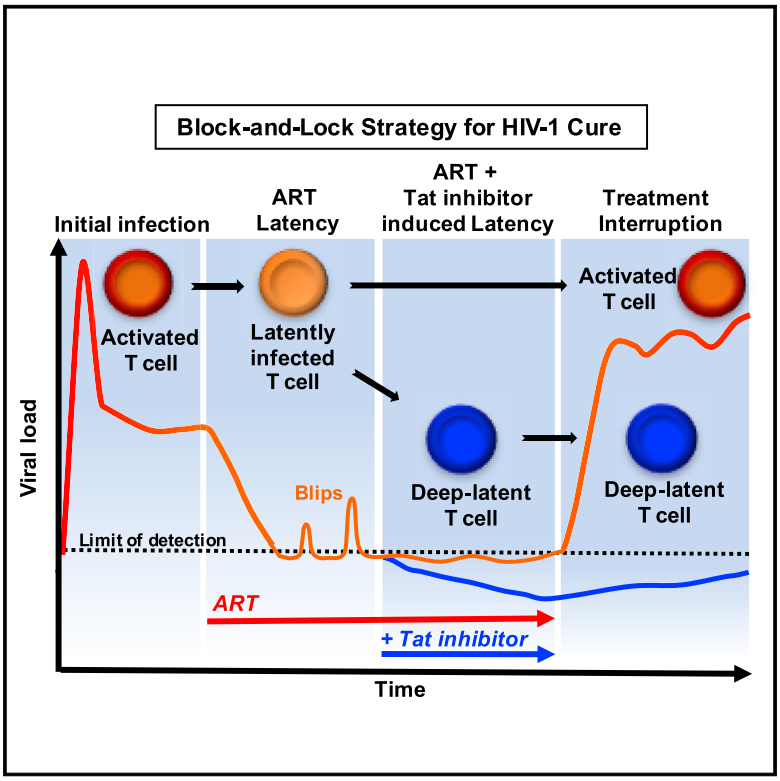

Highlights

- Didehydro-Cortistatin A (dCA) reduces HIV transcription and reactivation from latency
- dCA suppresses viral rebound after treatment interruption in HIV$^+$ humanized BLT mice
- dCA promotes epigenetic silencing of the HIV-1 promoter
- "Block-and-lock" approach is a viable alternative for a functional HIV cure

Authors

Cari F. Kessing, Christopher C. Nixon, Chuan Li, ..., Lydie Trautmann, J. Victor Garcia, Susana T. Valente

Correspondence

victor_garcia@med.unc.edu (J.V.G.), svalente@scripps.edu (S.T.V.)

In Brief

Tat inhibitors are amenable to functional cure approaches, which aim to reduce residual viremia during ART and limit viral rebound during treatment interruption. Using didehydro-Cortistatin A (dCA), Kessing et al. demonstrate the concept in human CD4$^+$ T cells from aviremic individuals and in the bone marrow-liver-thymus mouse model of HIV latency.

Kessing et al., 2017, Cell Reports *21*, 600–611
October 17, 2017
https://doi.org/10.1016/j.celrep.2017.09.080

OPEN ACCESS
CellPress

Cell Reports
Article

In Vivo Suppression of HIV Rebound by Didehydro-Cortistatin A, a "Block-and-Lock" Strategy for HIV-1 Treatment

Cari F. Kessing,[1,5] Christopher C. Nixon,[2,5] Chuan Li,[1,5] Perry Tsai,[2] Hiroshi Takata,[3,4] Guillaume Mousseau,[1] Phong T. Ho,[2] Jenna B. Honeycutt,[2] Mohammad Fallahi,[1] Lydie Trautmann,[3,4] J. Victor Garcia,[2,*] and Susana T. Valente[1,6,*]

[1]Department of Immunology and Microbiology, The Scripps Research Institute, Jupiter, FL, USA
[2]Division of Infectious Diseases, Center for AIDS Research, University of North Carolina, School of Medicine, Chapel Hill, NC, USA
[3]U.S. Military HIV Research Program, Walter Reed Army Institute of Research, Silver Spring, MD, USA
[4]Henry M. Jackson Foundation for the Advancement of Military Medicine, Bethesda, MD, USA
[5]These authors contributed equally
[6]Lead Contact
*Correspondence: victor_garcia@med.unc.edu (J.V.G.), svalente@scripps.edu (S.T.V.)
https://doi.org/10.1016/j.celrep.2017.09.080

SUMMARY

HIV-1 Tat activates viral transcription and limited Tat transactivation correlates with latency establishment. We postulated a "block-and-lock" functional cure approach based on properties of the Tat inhibitor didehydro-Cortistatin A (dCA). HIV-1 transcriptional inhibitors could block ongoing viremia during antiretroviral therapy (ART), locking the HIV promoter in persistent latency. We investigated this hypothesis in human CD4$^+$ T cells isolated from aviremic individuals. Combining dCA with ART accelerates HIV-1 suppression and prevents viral rebound after treatment interruption, even during strong cellular activation. We show that dCA mediates epigenetic silencing by increasing nucleosomal occupancy at Nucleosome-1, restricting RNAPII recruitment to the HIV-1 promoter. The efficacy of dCA was studied in the bone marrow-liver-thymus (BLT) mouse model of HIV latency and persistence. Adding dCA to ART-suppressed mice systemically reduces viral mRNA in tissues. Moreover, dCA significantly delays and reduces viral rebound levels upon treatment interruption. Altogether, this work demonstrates the potential of block-and-lock cure strategies.

INTRODUCTION

HIV persists in latently infected CD4$^+$ T cells in infected individuals even after prolonged periods on suppressive antiretroviral therapy (ART). Stable cellular reservoirs that harbor proviral DNA are thought to be the source of viremia upon ART interruption (Chun et al., 2008; Günthard et al., 2001; Søgaard et al., 2015). Continuous viral production from viral reservoirs and transcriptional reactivation from latently infected cells are not affected by current antiretrovirals (ARVs), highlighting the need for novel approaches to achieve such an end (Chun et al., 2008; Günthard et al., 2001; Søgaard et al., 2015).

The viral Tat protein binds HIV-1 mRNA and efficiently recruits the necessary transcriptional factors to the HIV promoter to initiate exponential viral transcription elongation (Dingwall et al., 1989, 1990; Kao et al., 1987; Toohey and Jones, 1989). Tat has no cellular homolog and is expressed early in the virus life cycle, making it an ideal target for therapeutic intervention. Inhibitors of Tat have been highly sought after, but none is yet in the clinic. We identified didehydro-Cortistatin A (dCA) as a specific and potent Tat inhibitor (Mousseau et al., 2012). Over time, dCA drives HIV-1 gene expression into a state of persistent latency, refractory to viral reactivation by the usual panel of latency reversal agents (LRAs) in cell lines and primary CD4$^+$ T cells isolated from infected individuals (Mousseau et al., 2015a). We postulated that this type of HIV-1-specific transcriptional inhibitors are amenable to a "block-and-lock" functional type approach to HIV-1 cure. Through increased epigenetic repression of the HIV promoter, Tat inhibitors could promote a durable state of latency, halting ongoing viral transcription during ART and blocking reactivation from latency (for example, in situations of therapy non-compliance, or blocking "blips" which are spontaneous reactivation events during ART), which may contribute to replenishment of the latent reservoir and continued persistence of HIV infection (Lorenzo-Redondo et al., 2016; Rong and Perelson, 2009).

The small number of latently infected cells in vivo has hindered studies of molecular mechanisms of HIV latency and reactivation. So far, no single primary cellular model alone accurately captures the response characteristics of latently infected T cells from patients because these use clonal HIV strains, cultivate CD4$^+$ T cells in cytokine cocktails that alter cell subset representation, or transform CD4$^+$ T cells to prolong lifespan. We used a cell culture approach that allows expansion of large numbers of primary CD4$^+$ T cells from successfully treated HIV-infected donors in the presence of ART (Trautmann et al., 2002, 2005; Van de Griend et al., 1984). Under these conditions, primary CD4$^+$ T cells carrying an autologous HIV reservoir proliferate for 2 weeks, return to a resting state after 3 weeks, and can

be maintained for up to 10 weeks. Cells stop producing HIV particles after 3 weeks, but the virus can be reinduced either upon drug interruption or upon stimulation with LRAs, all while preserving their in vivo representation of the HIV reservoir. Using this approach, we explored the long-term effects of a prior exposure to dCA on natural or induced viral rebound during treatment discontinuation. We previously showed the lasting inhibitory activity of dCA over a short 6 day treatment interruption period (Mousseau et al., 2015a). Here, we report that prior treatment with dCA inhibits viral rebound when treatment is interrupted for an extended 25-day period, even when cells were subjected to protein kinase C (PKC) activation or strong T cell receptor (TCR) signaling.

Repressive nucleosomes are associated with latent proviruses, and, upon reactivation from latency, rearrangement of the nucleosomal structure and loss of protection from Nucleosome-1 (Nuc-1) regions is observed (Rafati et al., 2011). To investigate the epigenetic profile at the HIV-1 promoter mediated by dCA, we took advantage of the previously described OM-10.1 HIV-1 latency model, in which we had established a state of sustained latency by dCA (Mousseau et al., 2015a). We used micrococcal nuclease (MNase) nucleosomal protection assays and chromatin immunoprecipitation (ChIP) to histone H3 to evaluate rearrangements of the nucleosomal structure. We observed higher nucleosomal occupancy (histone H3) at the Nuc-1 region and small changes in H3 occupancy upon transcriptional activation in dCA-treated cells. This result was supported by a drastic inhibition of RNA polymerase II (Pol II) recruitment to the HIV promoter and genome and, thus, inhibition of transcriptional elongation.

To evaluate the in vivo efficacy of dCA, we utilized the bone marrow-liver-thymus (BLT) mouse model of HIV-1 latency and persistence. Numerous studies have shown that BLT mice recapitulate key features of HIV infection, pathogenesis, and latency (Cheng et al., 2017; Denton et al., 2012; 2014; Garcia, 2016; Melkus et al., 2006; Zhen et al., 2017). Administration of dCA to ART-suppressed animals for a period of 2 weeks resulted in a general one-log loss of viral RNA in tissues. Furthermore, co-dosing of dCA with ART for a period of 4 weeks significantly delayed viral rebound and reduced viral rebound levels after all treatments were interrupted. These results demonstrate the activity of dCA in an in vivo model of HIV-1 infection and represent a strong proof of concept of the block-and-lock approach for the functional cure of HIV.

RESULTS

dCA Accelerates HIV-1 Suppression

HIV-infected memory $CD4^+$ T cells remain in a resting state in the presence of ART; however, periodic activation of cells is believed to occur in subjects on ART, contributing to the basal low levels of viremia. In cell models of latency, the virus can be reactivated either upon ART removal or upon cellular stimulation with HIV LRAs. To study the ability of dCA to limit viral transcription in these contexts, we used a previously established protocol to maintain primary $CD4^+$ T cells from infected individuals for up to 10 weeks in culture, while preserving their characteristic representation of the HIV reservoir (Kessing et al., 2017; Mousseau et al., 2015a).

Using this model, we previously reported dCA's block of viral rebound for a 6-day period after ART interruption. The question remained, though, whether this inhibitory activity was long-lasting and whether it could withstand strong cellular stimulation. Here we assessed the ability of dCA to promote transcriptional suppression for a period of 25 days while receiving strong T cell activation 7 days after treatment interruption. Peripheral blood mononuclear cells (PBMCs) from five HIV-infected subjects on suppressive ART for at least 3 years were collected, and $CD4^+$ T cells were isolated and expanded in the presence of interleukin-2 (IL-2) (100 U/mL), phytohemagglutinin (PHA) (1 μg/mL), and "feeder cells" (Figure 1A). Cells were then kept in culture for 60 days in medium containing IL-2 (20 U/mL) and ART (efavirenz, zidovudine, and raltegravir) and with or without 50 nM dCA ("ART" or "ART + dCA" conditions) (Figure 1B). Viral particle genomic RNA in the culture supernatant was quantified by ultrasensitive qRT-PCR every 7 days. After 21 days of treatment, virus production from all five subjects' cells exposed to dCA was below the limit of detection and significantly inhibited compared with ART alone ($p = 0.0238$) (Figure 1B). On day 35, supernatant HIV RNA levels from all subjects' cells were below detection and remained so until day 60 in both treatment groups. The amount of total integrated HIV DNA was measured over time. As expected, because of the presence of ART under both conditions, no significant differences in total HIV DNA content were observed between the cells immediately after isolation from the patients' blood, labeled ex vivo, and the expanded cells in ART or ART + dCA, up to day 42 (Figure 1C). Therefore, viral mRNA production in dCA-treated samples is the consequence of Tat transcriptional inhibition and not a reduction in proviral content. Moreover, because the total HIV DNA content between ex vivo cells and expanded ones is similar, the representation of each individual's viral reservoir is not being lost. However, on day 49, we observed a general loss of proviral DNA content following the cellular expansion performed on day 42. This is possibly due to some increased cytopathic effects associated with the age of the cells, reflecting some of the limitations of primary models. Nevertheless, the proviral content between the ART and the ART with dCA-treated cells remains similar, permitting comparisons of viral RNA expression.

dCA Limits Viral Reactivation after Stimulation

To determine the ability of dCA to effectively block viral rebound after strong nuclear factor κB (NF-κB) activation, cells were treated with the PKC activator, prostratin, in the absence of any treatment (Figure 1B, orange and pink arrows), on day 35, when viral RNA production was below detection in all groups. HIV RNA in the supernatant was measured by qRT-PCR 24 hr later. When ART was removed, followed by stimulation, viral rebound was immediately observed in all subjects' cells (Figure 1D, orange bars). In contrast, upon dCA + ART removal followed by stimulation, viral reactivation was inhibited by 96.3%, 100%, 100%, 99.4%, and 99.8% in cells from subjects A, B, C, D, and E, respectively, with an overall average inhibition of 99% for all five subjects after 24 hr (Figure 1D, pink bars). Upon prostratin treatment, viral reactivation in cells with prior

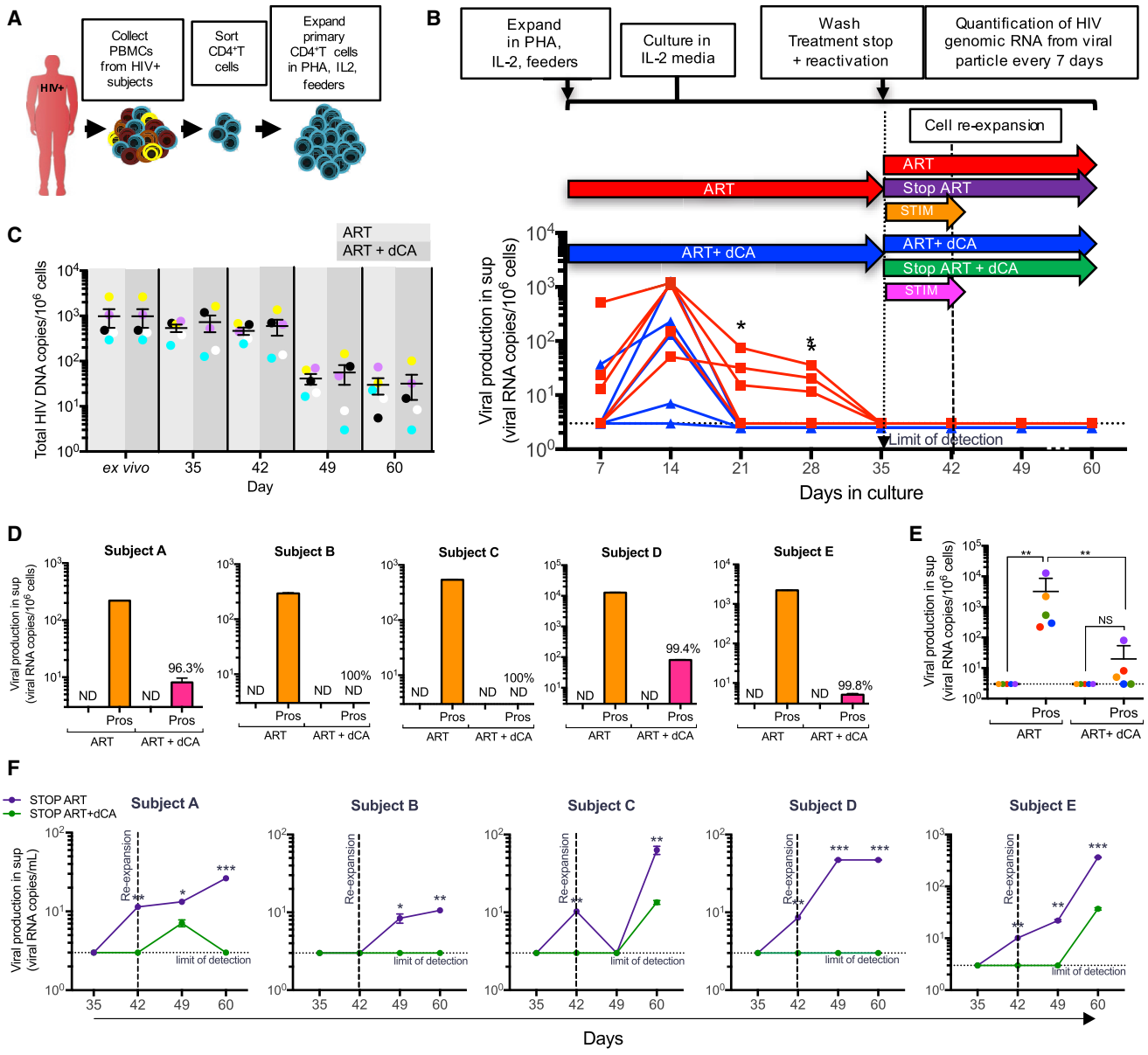

Figure 1. Addition of dCA to ART Promotes Rapid HIV-1 Suppression from Primary Human CD4⁺ T Cells Isolated from Infected Individuals and Inhibits Viral Rebound during Reactivation and Treatment Interruption

(A) PBMCs are extracted from successfully treated aviremic HIV-infected individuals (at least 3 years on ART). CD4⁺ T cells are isolated and expanded in PHA, IL-2, and feeder cells (irradiated PBMCs from 3 healthy donors).

(B) Expanded primary human CD4⁺ T cells from 5 HIV-infected individuals were kept on IL-2 alone and treated with a cocktail of ART with or without 50 nM dCA. Viral RNA levels in the supernatant of ART- and ART + dCA-treated cells were measured every 7 days. After 35 days in culture, viral RNA production in the supernatant was below the detection limit (*$p < 0.05$).

(C) Total HIV DNA was determined up to 60 days in cells treated with ART or ART + dCA. The limit of detection for qRT-PCR is 3 viral copies per million cells, and error bars represent SE.

(D) On day 35, cells were stimulated overnight with 1 μM prostratin without ART or dCA. Viral production in the supernatant was quantified by qRT-PCR. Error bars represent SD.

(E) Aggregate plot of data from (D). There was a significant decrease (**$p < 0.01$) in viral rebound after stimulation in dCA-treated mice compared with ART alone. Error bars represent SD.

(F) Treatment interruption does not result in immediate viral rebound even during strong cellular activation. On day 35, all drugs (ART and dCA) were removed, and viral output in the supernatant was quantified for the next 25 days by qRT-PCR. Cells were re-expanded with PHA, IL-2, and feeder cells on day 42 to maintain cell cultures and provide stimulation. The results show viral RNA levels in the supernatant for each individual sample. Error bars represent SD. *$p < 0.05$, **$p < 0.01$, ***$p < 0.001$. ND, not detected; sup, supernatant.

exposure to dCA was significantly reduced compared with cells treated with ART alone ($p = 0.008$), and no significant differences were observed in viral reactivation in dCA-treated cells before or after stimulation (Figure 1E). These results demonstrate that prior treatment with dCA (for 35 days) results in repression of viral promoter activity, a potentially effective treatment for preventing moments of viral reactivation under suppressive ART and replenishment of the reservoir in vivo.

dCA Treatment Prevents Viral Rebound after Therapy Interruption and Strongly Reduces Viral Rebound after Mitogenic Stimulation

ART interruption in HIV-suppressed individuals, in all but exceptional cases, results in viral rebound within weeks. To determine whether prior treatment with dCA could have lasting repressive transcriptional activity after treatment interruption, we stopped ART or ART + dCA on day 35 and followed viral replication in the supernatant by qRT-PCR for another 25 days (up to day 60) (Figures 1B, purple and green arrows, and 1F). Cells remaining on treatment showed no viral production after day 35 (Figure 1B, red and blue arrows). Seven days after treatment cessation, viral rebound was readily observed in 4 of the 5 subjects' cells treated with ART alone. No rebound was observed in $CD4^+$ T cells previously cultured in the presence of ART + dCA from all five subjects by day 7. Viral rebound was seen in all 5 ART-treated subjects' cells 25 days after treatment interruption, and only 2 rebounded minimally in cells previously treated with ART + dCA (Figure 1F). To assess whether dCA-mediated transcriptional suppression could withstand events of viral reactivation even in the absence of treatment, cells were activated on day 42 with PHA, IL-2, and feeder cells. In all ART-treated cells (no dCA), viral production continuously increased over time, whereas it was drastically inhibited in cells treated with ART + dCA. Our results clearly demonstrate that combining dCA with ART can potently inhibit viral reactivation from latency after treatment cessation even during strong cellular activation, suggesting that dCA contributes to long-lasting repression of the HIV promoter.

dCA Does Not Alter T Cell Activation Levels

The phenotype of the $CD4^+$ T cells treated with ART or ART + dCA was monitored weekly by flow cytometry up to day 49 to quantify the number of live cells and to ensure re-establishment of a resting state after expansion. We used $CD38^+$ as an activation marker and $CD127^+$ (IL-7 receptor) for quiescence (Figure S1A). Cells reached peak activation by day 14 after initial expansion, followed by a decrease in activation and return to a resting state. As expected, $CD38^+$ expression increased and $CD127^+$ expression decreased during peak activation. Cells were re-expanded on day 42, and expression of activation markers increased accordingly. Additionally, the viability of the cultures was measured by trypan blue staining over time during treatment and after treatment interruption (Figure S1B), and DNA content was measured before and after stimulation to ensure that there was no loss or variation of the number of infected cells between treatment groups (Figure S1C). Gene expression was also monitored using a biomark assay of 52 genes related to various signaling pathways, including T cell activation, cell cycle, apoptosis, transcription factors, and TCR signaling (Figure S2). No statistically significant differences were observed over time between the three individuals' cell samples and between treatments. Even when not significant, we observed the GATA3 and CCR7 genes to be the most altered between ART and ART + dCA samples on day 14. It has been reported that GATA3 and CCR7 expression is inversely correlated with HIV expression (Kessing et al., 2017; Ramirez et al., 2014; Rueda et al., 2012). Therefore, in future work, we will further investigate these genes during expansion of the cells in vitro.

Collectively, no significant differences in phenotype or gene expression were observed in cells treated with ART compared with ART + dCA over time. Our results suggest that long-term treatment of primary human $CD4^+$ T cells in vitro with dCA establishes a state of sustained latency that nearly or completely hinders the provirus capacity for reactivation after treatment removal without significantly affecting viability, phenotype, or cellular gene expression patterns.

Changes in Chromatin Signature and RNA Pol II Recruitment after dCA Treatment

Differential nucleosome organization in the HIV-1 long terminal repeat (LTR) correlates with transcription from proviral genomes in latently infected cells (Rafati et al., 2011). Our previous results suggested that dCA causes effects that promote the organization of repressive chromatin structure that prevents strongly/rapidly reactivating transcription of latent provirus. To examine the molecular correlates that control transcription from the HIV-1 promoter in response to long-term dCA treatment, we assayed histone density and chromatin accessibility as well as Pol II recruitment at the HIV-1 provirus using MNase digestion (Rafati et al., 2011) and ChIP in the previously described OM-10.1 HIV-1 latency model (Mousseau et al., 2015a). OM-10.1 cells contain a single copy of a fully replicative provirus and were treated with ART or ART + dCA until viral production was almost undetectable by p24 ELISA in dCA-treated samples (Figure 2A). On days 263, 276, and 286 (shown as circles and squares in Figure 2A), HIV-1 transcription was stimulated using the histone deacetylase (HDAC) inhibitor suberoylanilide hydroxamic acid (SAHA) (2.5 μM) for 8 hr in the presence of treatment, and cell-associated HIV-1 RNA was measured by qRT-PCR (Figure 2B). As expected, in OM-10.1 cells treated with ART + dCA, we observed 98% less viral rebound after SAHA treatment compared with cells treated with ART alone (Figure 2B). At these time points, unstimulated and SAHA-stimulated cells from each treatment condition were fixed with formaldehyde, and nuclei were prepared and treated with MNase under conditions to generate mono-nucleosomes. Under unstimulated conditions in OM10.1 cells, we detected MNase-protected regions at the 5′ end of the LTR (Nuc-0) and in two regions immediately downstream of the transcription start site (TSS), Nuc-1 and Nuc-2, as well as an MNase-sensitive region at the DNaseI-hypersensitive region (DHS-1) immediately upstream of the TSS (Figure 2C). MNase protection, and most likely nucleosomal occupancy, at Nuc-0 or Nuc-2 was similar in resting cells treated with ART compared with those treated with ART + dCA. However, there was significantly stronger MNase protection at Nuc-1 in cells treated with ART + dCA, suggesting increased

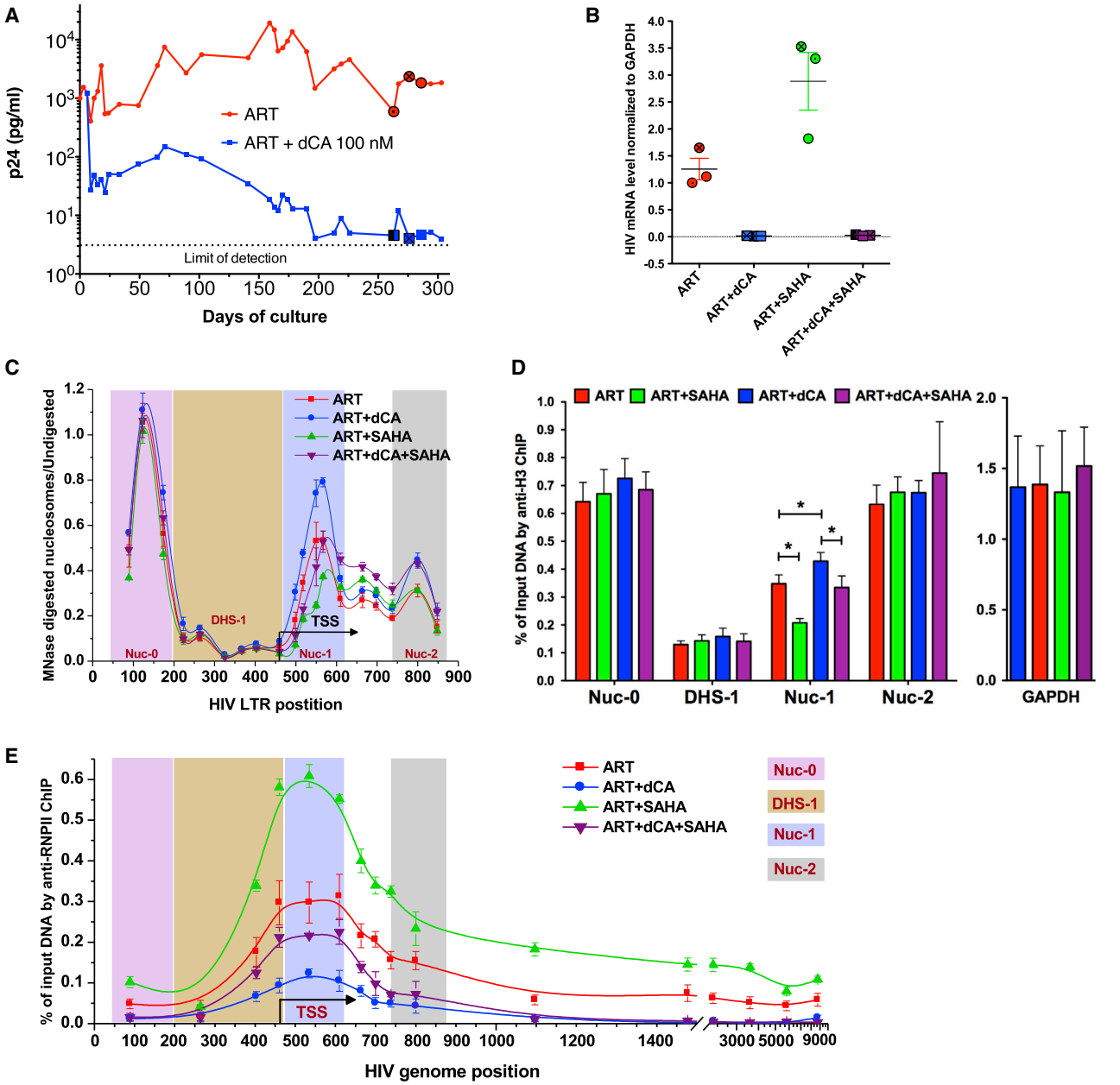

Figure 2. Characterization of Chromatin Structure and RNA Pol II Recruitment to the HIV Genome after Long-Term Treatment with dCA Using the OM10.1 Latency Model

(A) dCA inhibits viral production in the OM-10.1 cell line to almost undetectable levels. OM-10.1 cells were split and treated on average every 3 days in the presence of ARVs with or without dCA (100 nM). Capsid production was quantified via p24 ELISA. Data are representative of four independent experiments.

(B) On days 263, 276, and 286, cells treated with ARVs and ARVs + dCA (100 nM) were stimulated with SAHA (2.5 μM) for 8 hr (highlighted with ⊙/⊠ in (A)). cDNAs prepared from total RNA were quantified by qRT-PCR with Nef region primers. The results were normalized as the number of viral mRNA copies per glyceraldehyde 3-phosphate dehydrogenase (GAPDH) mRNA. Viral mRNA generated in the ARV control was set to 100%, and error bars represent the SDs of 3 independent experiments.

(C) The chromatin structure of the HIV LTR assessed by MNase protection assay. The chromatin profile of cell samples from (B) was determined by normalizing the amount of the MNase-digested PCR product to that of the undigested product using the ΔC(t) method (y axis), which is plotted against the midpoint of the corresponding PCR amplicon (x axis). The x axis represents base pair units, with 0 as the start of the HIV LTR. Error bars represent the SEM of 3 independent experiments.

(D) H3 ChIP of cell samples from (B). The promoter of GAPDH was used as a reference. The results are presented as percent immunoprecipitated DNA over input. Data are the average of 3 independent experiments, and error bars represent the SEM of 3 experiments for each primer set. Statistical significance was determined using paired t test; *$p < 0.05$.

(E) Distribution of Pol II on the HIV genome. ChIP to Pol II was performed using cell samples from (B). Data are the average of 3 independent experiments, and error bars represent the SEM of 3 experiments for each primer set.

nucleosome occupancy at this location in the presence of dCA (Figure 2C). After SAHA treatment, MNase protection decreased at Nuc-1 in both ART or ART + dCA-treated groups (Figure 2C). However, occupancy at Nuc-1 in cells treated with ART + dCA was comparable with that in unstimulated cells treated with ART alone. This suggests that a combination of dCA + ART decreases chromatin accessibility at the LTR, reducing the transcriptional competence of latent HIV-1 genomes under conditions that promote reactivation.

To determine whether increased MNase protection at the Nuc-1 region was likely due to increased nucleosome occupancy during treatment with dCA + ART, an antibody specific for total histone H3 was used in ChIP assays (Figure 2D). A significant increase in H3 at the Nuc-1 region was apparent in ART + dCA-treated cells compared to ART alone, whereas we did not observe differences in H3 occupancy at Nuc-0, DHS-1, and Nuc-2 between any of the samples (Figure 2D, red versus blue bars). Moreover, H3 occupancy at the Nuc-1 region in ART + dCA-treated samples after SAHA activation was comparable with that observed in ART-treated cells prior to activation (Figure 2D, red versus purple bars). Thus, although SAHA treatment reduced H3 occupancy at the Nuc-1 region in both SAHA-stimulated samples, the absolute amount of H3 coverage remained high in dCA + ART-treated cells. These results provide evidence that increased MNase protection at the Nuc-1 region in dCA-treated cells is the result of increased nucleosome occupancy.

Next we investigated the recruitment of Pol II to the HIV provirus using ChIP (Figure 2E). In cells treated with either ART alone or ART + dCA, there was a peak of Pol II near the HIV-1 promoter, but this peak was significantly lower in cells treated with dCA + ART (Figure 2E, compare red and blue lines). Thus, fewer HIV-1 proviruses have RNA Pol II recruited to their TSSs in the presence of dCA. Furthermore, cells treated with ART + dCA lacked detectable Pol II density within the transcribed portion of the HIV-1 genome, whereas cells treated with only ART exhibited a substantial Pol II signal. In the additional presence of SAHA, cells treated with either ART alone or ART + dCA both increased Pol II recruitment to the promoter (Figure 2E). However, recruitment in ART + dCA-treated samples after SAHA activation was lower than that observed in ART-treated cells prior to activation. Moreover, there was a striking absence of Pol II within the transcribed sequences of HIV-1 in cells treated with dCA + ART compared with cells treated with ART only. Taken together, our results indicate that extended inhibition of Tat activity with dCA treatment promotes increased nucleosome occupancy in the Nuc-1 region and that this precludes RNA pol II recruitment to the LTR and also reduces its elongation potential upon stimuli that normally induce HIV-1 transcription.

The Effect of dCA on Tissue Viremia in HIV-Infected, ART-Suppressed BLT Humanized Mice

We explored the activity of dCA in vivo by asking whether dCA administration would affect the levels of cell-associated viral RNA that persist in lymphoid tissues despite ART (Denton et al., 2014). We first determined that dCA had good pharmacokinetic properties in mice receiving once-daily intraperitoneal dosing at 0.50 mg/kg with no loss of body weight or adverse effects in blood biochemistry (data not shown). Next, BLT humanized mice (n = 14) were infected with HIV-1_{JRCSF} and bled weekly for the duration of the experiment to monitor plasma viral load and human $CD4^+$ T cells counts (Figure 3A). Two weeks following virus exposure, systemic infection was confirmed, and ART was initiated. Five weeks after the initiation of ART, vehicle or dCA (0.5 mg/kg) was administered for 14 days (n = 7 in each group). The copies of viral RNA per milliliter of plasma remained below our level of detection in all animals, and the levels of human $CD4^+$ T cell levels in peripheral blood were not affected by dCA (Figures 3B and 3C; Figure S3).

At the end of this period, mice were sacrificed, and tissues were harvested for analysis of viral RNA and human cells. Viral RNA levels were quantified by qRT-PCR and normalized to the number of human $CD4^+$ T cells in spleens, lymph nodes, bone marrow, and PBMCs (Figure 3D, left). In the lymph node, the mean number of copies of viral RNA per 10^5 $CD4^+$ T cells was 10.5-fold lower in dCA-treated mice compared with control mice (153.2 ± 63.28 versus 1614 ± 714.5), and this difference was statistically significant ($p = 0.0111$). The reductions in RNA levels observed in all other lymphoid tissues were not statistically significant. However, when these four lymphoid tissues were analyzed in aggregate, we found a statistically significant difference in the number of copies of viral RNA in dCA-treated mice compared with controls ($p = 0.0487$) (Figure 3D, right). The mean number of copies of viral RNA per 10^5 $CD4^+$ T cells in these combined tissues in dCA-treated BLT mice was 191.7 ± 49.93, whereas it was 725.6 ± 233.9 in the same tissues from control mice, indicating a 3.8-fold lower mean level of viral RNA in mice treated for 14 days with dCA. Analysis of HIV RNA levels in brains obtained from mice treated with dCA also showed a significant (~7-fold) decrease compared with control mice ($p = 0.0326$). In summary, these results indicate that dCA treatment does not negatively affect suppression of HIV-1 infection by ART or alter the levels of human $CD4^+$ T cells in BLT mice. Furthermore, there is a clear trend indicating lower levels of viral gene expression in dCA-treated, HIV-infected, ART-suppressed humanized mice compared with control mice treated with a saline control.

Effect of dCA Treatment on Viral Rebound Following Therapy Interruption

Next we asked whether dCA treatment would affect the kinetics of viral rebound upon therapy interruption. Therefore, we infected BLT humanized mice with HIV-1_{JRCSF}, and infection was confirmed 2 weeks post-exposure, at which point therapy was initiated (Figure 4A). After 3 weeks of ART, either dCA (n = 10) or vehicle (n = 8) treatment was combined with ART. At the end of 4 weeks of co-administration, both dCA and ART treatment were discontinued, and plasma viremia was monitored over time. During treatment, there were no discernible differences in the levels of human $CD4^+$ or $CD8^+$ T cells in peripheral blood between mice receiving ART + dCA and those receiving ART + vehicle (Figure S4).

Control mice began to exhibit rebound viremia as early as 3 days after therapy interruption, and by day 10, all eight control mice showed rebound viremia (Figures 4B and 4C). In stark contrast, none of the ten mice that received dCA treatment exhibited rebound viremia on day 3, and only one had detectable levels of plasma viremia by day 7. By day 10, all eight control

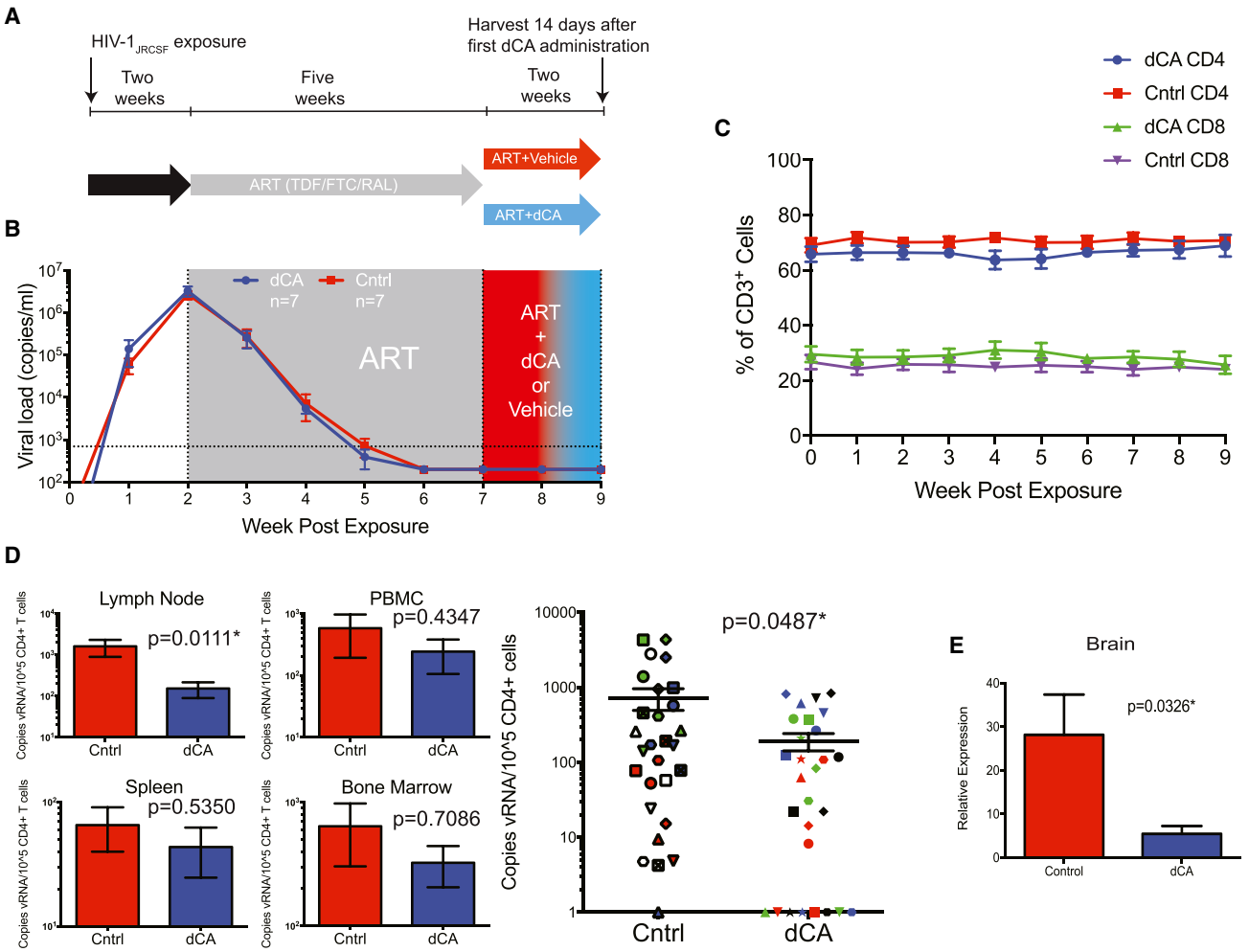

Figure 3. Effect of dCA on ART-Mediated Suppression of Viremia and Residual Viral RNA Expression in Tissues of Humanized Mice

(A) Diagram outlining the experimental design and highlighting the two different treatments (red and blue).

(B) Aggregate plot of all HIV-infected BLT humanized mice receiving dCA (blue, n = 7) or vehicle (red, n = 7) in addition to ART, showing similar kinetics of viral suppression and no increases in plasma viral load as a result of dCA treatment.

(C) dCA administration does not affect plasma viral load levels or the levels of $CD4^+$ or $CD8^+$ T cells in peripheral blood.

(D) Left: residual HIV-1 RNA levels in spleens, bone marrow, lymph nodes, and PBMCs from control (red) and dCA-treated mice (blue). Right: reductions in viral RNA for all individual tissues from all animals are graphed together. Each mouse was assigned a different shape, and tissues are coded by color: spleen, red; bone marrow, blue; lymph node, green; PBMC, black.

(E) Residual HIV-1 RNA levels in brain tissue from control and dCA-treated animals. HIV RNA levels were normalized to the levels of TATA box binding protein RNA.

The error bars in (D) and (E) indicate SEM. Statistical significance was determined using Mann-Whitney *U* test.

mice continued to show high levels of plasma viremia. In contrast, the virus was still below detection in 6 of 10 dCA-treated mice. Indeed, on days 13 and 16, no additional dCA-treated mice exhibited rebound viremia. It was not until day 19 after therapy interruption that viral rebound was first detected in the remaining five dCA-treated mice (Figures 4B and 4C).

When the means of the rebound viremia in control mice were compared with those of the dCA-treated mice, there were statistically significant differences between the two groups beginning on day 7 and for each time point thereafter (Figure 4D; Table 1) (Mann-Whitney *U* test). On day 7, the difference in mean viremia between control and dCA-treated mice was 1,085 copies of viral RNA/mL of plasma (1,500 copies of viral RNA/mL in control versus 410 in dCA-treated mice, p = 0.0091). On day 10, the mean viral load of the control mice was greater than 2×10^5 compared with only 3×10^3 copies of viral RNA/mL plasma in the dCA-treated mice. This is a difference of greater than 2×10^5 copies of viral RNA/mL plasma (p = 0.0067). The difference in the means of viral loads at day 13 was greater that $5x10^5$ copies of viral RNA/ml plasma (p = 0.0243). The largest difference between the viral loads of control mice and dCA-treated mice (120-fold, p = 0.0029) was noted on day 16 after therapy interruption. Even on day 19 after therapy interruption, a 5-fold difference in plasma viral loads was observed (p = 0.0198)

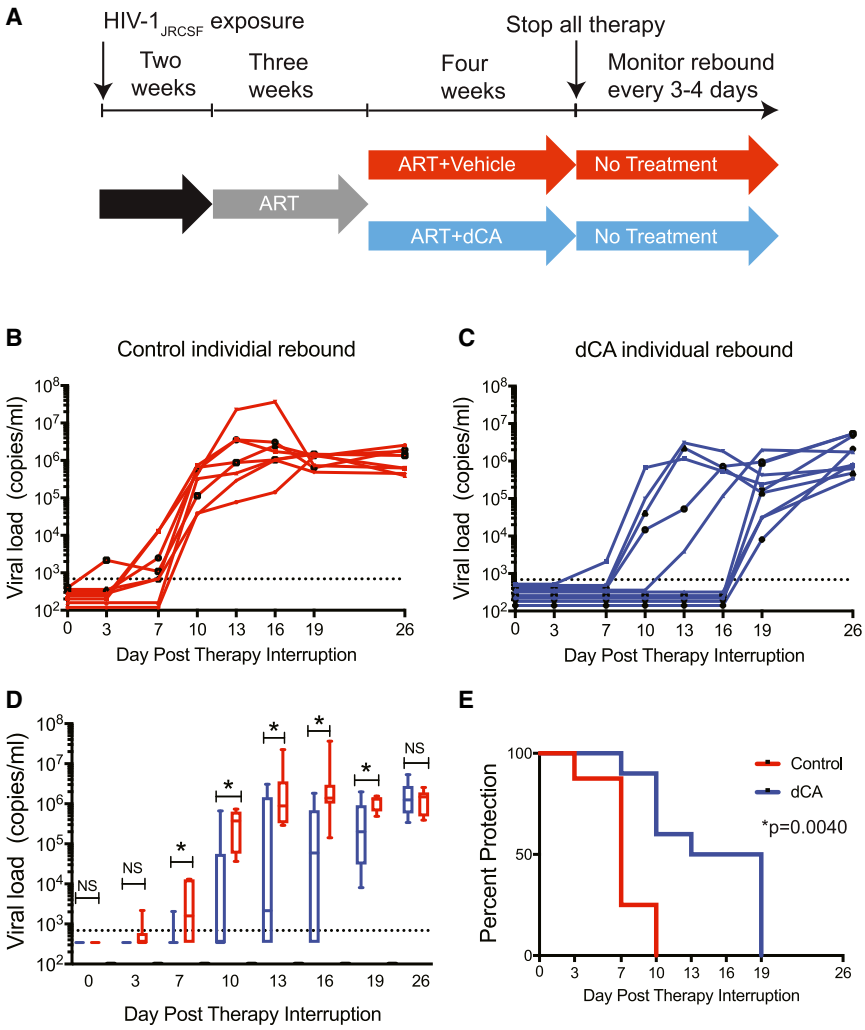

Figure 4. dCA Treatment Results in a Delay in Rebound Viremia in HIV-1-Infected, Suppressed BLT Humanized Mice following Therapy Interruption

(A) Diagram outlining the experimental design and experimental groups receiving ART + dCA (blue) or ART alone (red).

(B and C) Rebound viremia following therapy interruption (day 0) in individual HIV-infected ART-treated mice administered vehicle (B) or rebound viremia following therapy interruption (day 0) in individual HIV-infected, ART-treated mice that were administered dCA (C).

(D) Comparison of the median viral load of mice treated with vehicle and with dCA following therapy interruption. In these plots, the boxes extend from the first to the third quartiles, enclosing the middle 50% of the data. The middle line within each box indicates the median of the data. Blue boxes indicate dCA-treated mice, and red boxes indicate control mice. * indicates statistical significant differences between control and dCA-treated mice, as determined by Mann-Whitney *U* test.

(E) Time to event (Kaplan-Meier) plot demonstrating the significant delay in viral rebound observed in animals treated with dCA ($p = 0.0040$, exact rank test).

(Figure 4D; Table 1). It was not until day 26 after therapy interruption that the mean viral loads between the two groups were no longer different ($p = 0.7796$) (Figure 4D; Table 1). Time to event statistical analysis demonstrates that the differences in the time to rebound for all the mice in the dCA treatment and control groups is significantly different ($p = 0.0040$, exact rank test) (Figure 4E). Together, these results demonstrate that dCA treatment can significantly delay and reduce viral rebound in HIV-infected, ART-suppressed humanized mice.

DISCUSSION

Using two state-of-the-art models of HIV-1 latency and persistence, primary $CD4^+$ T cells isolated from infected ART-suppressed individuals and BLT humanized mice, our findings provide evidence that the Tat inhibitor dCA can potently inhibit residual levels of HIV viral transcription during suppressive ART and block viral reactivation upon stimulation or during treatment interruption.

The small number of latently infected cells in patients (~1 in 10^6 $CD4^+$ T cells) has complicated studies of HIV latency and reactivation (Pierson et al., 2000). To overcome this limitation, we utilized a method where memory $CD4^+$ T cells are isolated from aviremic HIV-infected subjects and expanded in vitro in the presence of ART, feeder cells, IL-2, and PHA (Trautmann et al., 2002, 2005; Van de Griend et al., 1984). In this primary cell system, using $CD4^+$ T cells from five infected, aviremic individuals, we answered several questions regarding the long-term in vitro activity of dCA. Does dCA have an additive activity to ART in reducing viral replication during cellular expansion? Does pretreatment of cells with dCA result in long-term suppression of the HIV promoter after treatment interruption, even when cells are subjected to strong cellular activation? Our results demonstrate the ability of dCA to accelerate the inhibition of viral production during cellular expansion compared with treatment with ART alone (Figure 1B), demonstrating the additive activity of dCA and supporting the notion that adding Tat inhibitors to frontline treatment might lead to faster suppression and potentially reduce the size of the established reservoir. Previous studies, in which infected individuals received ART within a few weeks of contracting HIV, found that this early treatment reduced total HIV DNA levels by 20-fold after a couple of weeks and showed a 316-fold reduction after 3 years (Ananworanich et al., 2015, 2016). Smaller reservoir sizes have also been linked to delays in viral load rebound after ART cessation (Hatzakis et al., 2004). For instance, this was observed in the case of a Mississippi baby (Persaud et al., 2013), the viro-immunological sustained control after treatment interruption

Table 1. Viral Load Analysis following Therapy Interruption in HIV-1-Infected ART-Suppressed BLT Humanized Mice Receiving Vehicle (Controls) or dCA

Days after Therapy Interruption	Viral Load of dCA-Treated Mice	Viral Load of Control Mice	Difference in Viral Load between Control and dCA-Treated Mice	Fold Difference in Viral Load between Control and dCA-Treated Mice	Mann-Whitney p Value
0	344	344	0	0	> 0.9999
3	344	433	90	1	0.4444
7	411	1,496	1,085	4	0.0091
10	3,028	222,705	219,677	74	0.0067
13	9,772	565,468	555,696	58	0.0243
16	13,865	1,722,890	1,709,025	125	0.0029
19	177,190	1,023,500	846,310	6	0.0198
26	1,254,213	1,489,199	234,987	1	0.7796

(VISCONTI) cohort (Hatzakis et al., 2004; Sáez-Cirión et al., 2013), and a French teenager (Frange et al., 2016).

Using primary cells from patients, we demonstrated the ability of dCA to inhibit reactivation from latency, exemplified by drastically impaired viral rebound upon cellular stimulation with the PKC activator, prostratin, after ART and dCA treatment interruption (Figures 1D–1F). The effects of dCA are solely correlated to inhibition of viral transcription because the total HIV DNA content remained unchanged throughout the study (Figure 1C; Figure S1C). It is important to ensure, in primary latency models, the maintenance of the representation of the individuals' viral reservoir over time and that there is no selection of a population of cells that is non-responsive to reactivating stimuli. In our model, we successfully demonstrated that the total proviral content before and after expansion was similar and that we had not lost cells with the ability to reactivate the virus, as observed in similar models (Bui et al., 2017).

The lasting activity of dCA to mediate long-term repression of the HIV promoter was shown by demonstrating its ability to limit viral rebound after treatment cessation. ART is known to successfully reduce viral replication in patients, but when ART is interrupted, HIV rebounds within weeks (Bennett et al., 2008; Davey et al., 1999). Using our primary cell system to recapitulate what is seen in patients, we demonstrated viral rebound within a week after treatment cessation in cells previously treated with ART alone for 35 days (Figure 1F). However, previous treatment with dCA drastically reduced viral rebound in primary human $CD4^+$ T cells after treatment cessation up to 25 days. Most importantly, when an extremely strong activation of the cells was performed using PHA, IL-2, and feeder cells, 7 days after treatment interruption, no viral rebound was observed in the cells pretreated with dCA.

Using the previously described OM10.1 cell line model of latency, we present evidence that dCA treatment results in a less permissive chromatin environment downstream of the TSS at Nuc-1 (Figure 2). This correlated with decreased Pol II recruitment and elongation. Upon activation of the cells with a latency-reversing agent such as SAHA, we observed a decrease in nucleosome occupancy at Nuc-1 and some increase in Pol II recruitment. However, recruited Pol II does not efficiently elongate to transcribe the full-length genome because this function is promoted by Tat. Therefore, HIV-1 mRNA transcription is drastically impaired even after stimulation, supporting previous studies that show that Tat is the master regulator of latency and the key switch to turn transcription on/off independent of cell activation status (Razooky et al., 2015). Collectively, our results suggest that dCA reduces HIV-1 transcriptional activity compared with what occurs under ART, promotes silencing of its promoter and reduces its potential for reactivation. Future studies will investigate how recruitment of specific cellular activators and repressors to the HIV-1 LTR/promoter regulates its epigenetic configurations and transcriptional potential in response to prolonged dCA treatment.

The efficacy of dCA in vivo was shown using the BLT humanized mouse model validated for the analysis of HIV latency and persistence (Cheng et al., 2017; Denton et al., 2012, 2014; Garcia, 2016; Melkus et al., 2006; Zhen et al., 2017). Humanized BLT mice are an excellent model for evaluating HIV latency because they allow us to track HIV infection of human cells, in the context of a complex substrate that includes mature T and B lymphocytes, monocytes, macrophages, and dendritic cells, because they infiltrate all organs and tissues in a living organism. Treatment with dCA reduced the levels of cell-associated viral RNA in lymphoid tissues. Most striking was the 10.5-fold reduction in the lymph node (Figure 3D). When analyzing all tissues combined, we observed an approximate 1-log reduction in systemic levels of viral RNA in a period of just 2 weeks (Figure 3D). Also impressive was the strong reduction in HIV RNA levels observed in the brains of dCA-treated mice. HIV infection of the brain has long been considered of paramount importance in HIV cure research. Recent reports indicate that the use of kick-and-kill approaches to HIV eradication might have negative consequences because they might increase immune activation, which could result in harmful inflammatory responses (Gama et al., 2017). Our results indicate that dCA and the block-and-lock approach to HIV cure might provide an important alternative of great significance. Given the feedback nature of the Tat-trans-activation response element (TAR) activity, and as shown previously (Mousseau et al., 2015a), the longer the treatment with dCA, the better the outcome because the promoter becomes increasingly silenced (Figure 2). This argues that we can only expect better outcomes with longer treatment periods with dCA. These results also support our findings in vitro, in which dCA accelerated entry of HIV into latency (Figure 1B).

The key experiment assessing the long-lasting activity of dCA in repressing HIV promoter transcription was performed in suppressed mice after 4-week coadministration of ART with dCA, followed by analytical treatment interruption (Figure 4). Virus was readily detected in the plasma of all mice receiving ART within 7 days after discontinuation of treatment. Impressively, in BLT mice previously treated with ART + dCA, viral rebound was significantly delayed up to 19 days after treatment interruption. It is worth noting that, in half of the dCA-treated mice, the virus was below our level of detection until day 16 after treatment interruption, only rebounding on day 19. In a general manner, dCA offered an impressive 9-day protection compared with ART alone. Future studies will investigate the relationship between the period of treatment with dCA to time to viral rebound. We speculate that, over time (in combination or not with other inhibitors), transcriptional repression could be pushed past a certain threshold where viral reactivation from latency is extremely difficult to overcome (Weinberger and Weinberger, 2013; Weinberger et al., 2008), blocking and locking HIV into sustained latency. Our results are the in vivo proof of principle for a block-and-lock approach for a functional cure of HIV. An additional benefit of HIV transcriptional inhibitors, whether they target Tat or TAR, or other factors, such as CDK9 or Cyclin T1 (reviewed in Mousseau et al., 2015b), is their ability to reduce morbidities associated with persistent levels of immune activation caused by low-level ongoing virus replication in subjects on suppressive ART (Hunt, 2010). Although controversial, a potential contributor to the sustained maintenance of the latent reservoir is viral replication reflected in blips observed in plasma that could be reseeding the reservoir even in the presence of ART (Chun et al., 2005; Jones and Perelson, 2007; Ramratnam et al., 2004). Additionally, therapy non-compliance or short breaks in therapy can also result in viral production and in reservoir replenishment. Including dCA in ART regimens could potentially inhibit reservoir replenishment during these situations.

In conclusion, we have demonstrated that, in the setting of full ART suppression of HIV, dCA reduces cell-associated viral RNA systemically, significantly delays viral rebound upon treatment interruption, and reduces viral rebound levels by several orders of magnitude. This is the first time pharmacological inhibition of viral rebound after treatment interruption has been shown in an in vivo model of HIV infection. These results strongly support the rationale for the inclusion of specific HIV transcriptional inhibitors in eradication strategies.

EXPERIMENTAL PROCEDURES

Subject Samples

Primary human $CD4^+$ T cells were collected from five HIV-seropositive subjects on stable suppressive ART for at least 3 years. All subjects provided signed informed consent approved by the Research Centre of the Centre Hospitalier de l'Université de Montréal (CR-CHUM) hospital (Montreal, Quebec, Canada) review boards. All patients underwent leukapheresis to collect large numbers of PBMCs.

Generation of Expanded Primary Human $CD4^+$ T Cells

Primary $CD4^+$ T cells from five successfully treated donors were expanded as described previously (Mousseau et al., 2015a). Briefly, 50×10^6 PBMCs were thawed, and sorted $CD45RA^-$, $CD27^+$, $CD4^+$ T cells were expanded with 1 μg/mL of PHA (Sigma-Aldrich), 100 U/mL of IL-2 (Roche), and irradiated feeder PBMCs (OneBlood). Cells were then kept on either ART alone (100 nM efavirenz, 180 nM zidovudine, and 200 nM raltegravir) or ART + 50 nM dCA (kindly provided by Dr. Phil Baran, Scripps La Jolla) in medium supplemented with human serum and 20 U/mL IL-2. ART reagents were obtained through the NIH AIDS Reagent Program, Division of AIDS, NIAID, NIH. For stimulation experiments, 1 million cells from each treatment group were isolated on day 35, treatments were washed away, and cells were stimulated with 1 μM prostratin (Sigma-Aldrich) overnight. Approximately 16 hr later, supernatants and cell pellets were collected for PCR.

Construction of Humanized BLT Mice

BLT humanized mice were prepared as described previously (Denton et al., 2008, 2011, 2012; Melkus et al., 2006). Briefly, a 1- to 2-mm piece of human liver tissue was sandwiched between two pieces of autologous thymus tissue (Advanced Bioscience Resources) under the kidney capsule of sublethally irradiated (300 cGy) 6- 8-week-old NOD.Cg-*Prkdc*^{scid} *Il2rg*^{tm1Wjl}/SzJ (NSG, The Jackson Laboratory) mice. Following implantation, mice were transplanted intravenously with hematopoietic $CD34^+$ stem cells isolated from autologous human liver tissue. Human immune cell reconstitution was monitored in the peripheral blood of BLT mice by flow cytometry every 3–4 weeks. Mice were maintained under specific pathogen-free conditions by the Division of Laboratory Animal Medicine at the University of North Carolina, Chapel Hill. Animal experiments were conducted in accordance with NIH guidelines for the housing and care of laboratory animals and in accordance with protocols reviewed and approved by the Institutional Animal Care and Use Committee at the University of North Carolina, Chapel Hill. For the study that examined the effect of dCA on residual tissue viremia under ART, the mean weight of the mice used was 27.18 g, and they were 11 months old. For the study that examined the effect of dCA on viral rebound following therapy interruption, the mean weight of the mice used was 26.31 g, and the mice were between 7 and 9 months old. All mice used in these studies were female.

Production of Viral Stocks for Infection of BLT Mice

Stocks of HIV-1_{JRCSF} were prepared as described previously (Wahl et al., 2012). Briefly, the proviral clone was transfected into HEK293T cells using Lipofectamine 2000 (Invitrogen) following the manufacturer's protocols. Viral supernatant was collected 48 hr after transfection. Viral supernatant was titered by infecting TZM-bl cells at multiple dilutions. Virus-containing medium was removed the next day and replaced with fresh DMEM plus 10% fetal bovine serum, and the incubation continued for 24 hr. The cells were fixed and stained with 5-bromo-4-chloro-3-indolyl-β-d-galactopyranoside, and blue cells were counted directly to determine infectious particles per milliliter. Each titer of these viral stocks was performed in triplicate, and at least two different titer determinations were performed for each batch of virus.

Statistical Analysis

The p values for in vitro experiments were calculated using one-way ANOVA and Kruskal-Wallis with post hoc Dunn multiple comparisons analysis or paired t test with 95% confidence intervals using Prism 7 for Macintosh (GraphPad). All in vivo statistical analyses were also performed in Prism 7. A two-tailed Mann-Whitney *U* test was used to compare levels of viral RNA in dCA-treated mice with control vehicle-treated mice.

SUPPLEMENTAL INFORMATION

Supplemental Information includes Supplemental Experimental Procedures, four figures, and one table and can be found with this article online at https://doi.org/10.1016/j.celrep.2017.09.080.

AUTHOR CONTRIBUTIONS

Investigation, C.F.K., C.C.N., C.L., P.T.H., and P.T.; Methodology, C.F.K., C.C.N., C.L., H.T., G.M., J.V.G., L.T., M.F., P.T.H., and J.B.H.; Conceptualization and Validation, C.F.K., C.C.N., J.V.G., and S.T.V.; Writing and Revisions, C.F.K., C.C.N., S.T.V., and J.V.G.; Funding Acquisition, S.T.V.; Resources, J.V.G. and S.T.V.; Supervision, J.V.G. and S.T.V.

ACKNOWLEDGMENTS

This work was supported by NIH Grants R01AI097012 and R01AI118432 and the Campbell Foundation (to S.T.V.) and MH108179 and AI-111899 (to J.V.G.). The research in this publication was also funded by CARE, a Martin Delaney Collaboratory, the National Institute of Allergy and Infectious Disease, National Institute of Neurological Disorders and Stroke (NINDS), National Institute on Drug Abuse (NIDA), and the National Institute of Mental Health (NIMH) of the NIH, grant number 1UM1AI126619. The content is solely the responsibility of the authors and does not necessarily represent the official views of the NIH. We thank Michael Hudgens, Camden Bay, and Katie Mollan (UNC CFAR Statistical Core, P30 AI050410) for performing the statistical analysis presented in Table 1 and Bonnie Howell and Stephanie Barrett (Merck & Co.) for providing antiretroviral-containing chow. We also thank former and current members of the Garcia laboratory and the husbandry technicians at the UNC Division of Laboratory Animal Medicine for their assistance.

Received: March 9, 2017
Revised: September 5, 2017
Accepted: September 25, 2017
Published: October 17, 2017

REFERENCES

Ananworanich, J., Dubé, K., and Chomont, N. (2015). How does the timing of antiretroviral therapy initiation in acute infection affect HIV reservoirs? Curr. Opin. HIV AIDS *10*, 18–28.

Ananworanich, J., Chomont, N., Eller, L.A., Kroon, E., Tovanabutra, S., Bose, M., Nau, M., Fletcher, J.L., Tipsuk, S., Vandergeeten, C., et al.; RV217 and RV254/SEARCH010 study groups (2016). HIV DNA Set Point is Rapidly Established in Acute HIV Infection and Dramatically Reduced by Early ART. EBioMedicine *11*, 68–72.

Bennett, D.E., Bertagnolio, S., Sutherland, D., and Gilks, C.F. (2008). The World Health Organization's global strategy for prevention and assessment of HIV drug resistance. Antivir. Ther. (Lond.) *13* (*Suppl 2*), 1–13.

Bui, J.K., Halvas, E.K., Fyne, E., Sobolewski, M.D., Koontz, D., Shao, W., Luke, B., Hong, F.F., Kearney, M.F., and Mellors, J.W. (2017). Ex vivo activation of CD4+ T-cells from donors on suppressive ART can lead to sustained production of infectious HIV-1 from a subset of infected cells. PLoS Pathog. *13*, e1006230.

Cheng, L., Ma, J., Li, J., Li, D., Li, G., Li, F., Zhang, Q., Yu, H., Yasui, F., Ye, C., et al. (2017). Blocking type I interferon signaling enhances T cell recovery and reduces HIV-1 reservoirs. J. Clin. Invest. *127*, 269–279.

Chun, T.W., Nickle, D.C., Justement, J.S., Large, D., Semerjian, A., Curlin, M.E., O'Shea, M.A., Hallahan, C.W., Daucher, M., Ward, D.J., et al. (2005). HIV-infected individuals receiving effective antiviral therapy for extended periods of time continually replenish their viral reservoir. J. Clin. Invest. *115*, 3250–3255.

Chun, T.W., Nickle, D.C., Justement, J.S., Meyers, J.H., Roby, G., Hallahan, C.W., Kottilil, S., Moir, S., Mican, J.M., Mullins, J.I., et al. (2008). Persistence of HIV in gut-associated lymphoid tissue despite long-term antiretroviral therapy. J. Infect. Dis. *197*, 714–720.

Davey, R.T., Jr., Bhat, N., Yoder, C., Chun, T.W., Metcalf, J.A., Dewar, R., Natarajan, V., Lempicki, R.A., Adelsberger, J.W., Miller, K.D., et al. (1999). HIV-1 and T cell dynamics after interruption of highly active antiretroviral therapy (HAART) in patients with a history of sustained viral suppression. Proc. Natl. Acad. Sci. USA *96*, 15109–15114.

Denton, P.W., Estes, J.D., Sun, Z., Othieno, F.A., Wei, B.L., Wege, A.K., Powell, D.A., Payne, D., Haase, A.T., and Garcia, J.V. (2008). Antiretroviral preexposure prophylaxis prevents vaginal transmission of HIV-1 in humanized BLT mice. PLoS Med. *5*, e16.

Denton, P.W., Othieno, F., Martinez-Torres, F., Zou, W., Krisko, J.F., Fleming, E., Zein, S., Powell, D.A., Wahl, A., Kwak, Y.T., et al. (2011). One percent tenofovir applied topically to humanized BLT mice and used according to the CAPRISA 004 experimental design demonstrates partial protection from vaginal HIV infection, validating the BLT model for evaluation of new microbicide candidates. J. Virol. *85*, 7582–7593.

Denton, P.W., Olesen, R., Choudhary, S.K., Archin, N.M., Wahl, A., Swanson, M.D., Chateau, M., Nochi, T., Krisko, J.F., Spagnuolo, R.A., et al. (2012). Generation of HIV latency in humanized BLT mice. J. Virol. *86*, 630–634.

Denton, P.W., Long, J.M., Wietgrefe, S.W., Sykes, C., Spagnuolo, R.A., Snyder, O.D., Perkey, K., Archin, N.M., Choudhary, S.K., Yang, K., et al. (2014). Targeted cytotoxic therapy kills persisting HIV infected cells during ART. PLoS Pathog. *10*, e1003872.

Dingwall, C., Ernberg, I., Gait, M.J., Green, S.M., Heaphy, S., Karn, J., Lowe, A.D., Singh, M., Skinner, M.A., and Valerio, R. (1989). Human immunodeficiency virus 1 tat protein binds trans-activation-responsive region (TAR) RNA in vitro. Proc. Natl. Acad. Sci. USA *86*, 6925–6929.

Dingwall, C., Ernberg, I., Gait, M.J., Green, S.M., Heaphy, S., Karn, J., Lowe, A.D., Singh, M., and Skinner, M.A. (1990). HIV-1 tat protein stimulates transcription by binding to a U-rich bulge in the stem of the TAR RNA structure. EMBO J. *9*, 4145–4153.

Frange, P., Faye, A., Avettand-Fenoël, V., Bellaton, E., Descamps, D., Angin, M., David, A., Caillat-Zucman, S., Peytavin, G., Dollfus, C., et al.; ANRS EPF-CO10 Pediatric Cohort and the ANRS EP47 VISCONTI study group (2016). HIV-1 virological remission lasting more than 12 years after interruption of early antiretroviral therapy in a perinatally infected teenager enrolled in the French ANRS EPF-CO10 paediatric cohort: a case report. Lancet HIV *3*, e49–e54.

Gama, L., Abreu, C.M., Shirk, E.N., Price, S.L., Li, M., Laird, G.M., Pate, K.A., Wietgrefe, S.W., O'Connor, S.L., Pianowski, L., et al.; LRA-SIV Study Group (2017). Reactivation of simian immunodeficiency virus reservoirs in the brain of virally suppressed macaques. AIDS *31*, 5–14.

Garcia, J.V. (2016). In vivo platforms for analysis of HIV persistence and eradication. J. Clin. Invest. *126*, 424–431.

Günthard, H.F., Havlir, D.V., Fiscus, S., Zhang, Z.Q., Eron, J., Mellors, J., Gulick, R., Frost, S.D., Brown, A.J., Schleif, W., et al. (2001). Residual human immunodeficiency virus (HIV) Type 1 RNA and DNA in lymph nodes and HIV RNA in genital secretions and in cerebrospinal fluid after suppression of viremia for 2 years. J. Infect. Dis. *183*, 1318–1327.

Hatzakis, A.E., Touloumi, G., Pantazis, N., Anastassopoulou, C.G., Katsarou, O., Karafoulidou, A., Goedert, J.J., and Kostrikis, L.G. (2004). Cellular HIV-1 DNA load predicts HIV-RNA rebound and the outcome of highly active antiretroviral therapy. AIDS *18*, 2261–2267.

Hunt, P.W. (2010). Th17, gut, and HIV: therapeutic implications. Curr. Opin. HIV AIDS *5*, 189–193.

Jones, L.E., and Perelson, A.S. (2007). Transient viremia, plasma viral load, and reservoir replenishment in HIV-infected patients on antiretroviral therapy. J. Acquir. Immune Defic. Syndr. *45*, 483–493.

Kao, S.Y., Calman, A.F., Luciw, P.A., and Peterlin, B.M. (1987). Anti-termination of transcription within the long terminal repeat of HIV-1 by tat gene product. Nature *330*, 489–493.

Kessing, C.F., Spudich, S., Valcour, V., Cartwright, P., Chalermchai, T., Fletcher, J.L., Takata, H., Nichols, C., Josey, B.J., Slike, B., et al. (2017). High Number of Activated CD8+ T Cells Targeting HIV Antigens Are Present in Cerebrospinal Fluid in Acute HIV Infection. J. Acquir. Immune Defic. Syndr. *75*, 108–117.

Lorenzo-Redondo, R., Fryer, H.R., Bedford, T., Kim, E.Y., Archer, J., Pond, S.L.K., Chung, Y.S., Penugonda, S., Chipman, J., Fletcher, C.V., et al. (2016). Persistent HIV-1 replication maintains the tissue reservoir during therapy. Nature *530*, 51–56.

Melkus, M.W., Estes, J.D., Padgett-Thomas, A., Gatlin, J., Denton, P.W., Othieno, F.A., Wege, A.K., Haase, A.T., and Garcia, J.V. (2006). Humanized mice mount specific adaptive and innate immune responses to EBV and TSST-1. Nat. Med. *12*, 1316–1322.

Mousseau, G., Clementz, M.A., Bakeman, W.N., Nagarsheth, N., Cameron, M., Shi, J., Baran, P., Fromentin, R., Chomont, N., and Valente, S.T. (2012).

An analog of the natural steroidal alkaloid cortistatin A potently suppresses Tat-dependent HIV transcription. Cell Host Microbe *12*, 97–108.

Mousseau, G., Kessing, C.F., Fromentin, R., Trautmann, L., Chomont, N., and Valente, S.T. (2015a). The Tat Inhibitor Didehydro-Cortistatin A Prevents HIV-1 Reactivation from Latency. MBio *6*, e00465.

Mousseau, G., Mediouni, S., and Valente, S.T. (2015b). Targeting HIV transcription: the quest for a functional cure. Curr. Top. Microbiol. Immunol. *389*, 121–145.

Persaud, D., Gay, H., Ziemniak, C., Chen, Y.H., Piatak, M., Jr., Chun, T.W., Strain, M., Richman, D., and Luzuriaga, K. (2013). Absence of detectable HIV-1 viremia after treatment cessation in an infant. N. Engl. J. Med. *369*, 1828–1835.

Pierson, T., McArthur, J., and Siliciano, R.F. (2000). Reservoirs for HIV-1: mechanisms for viral persistence in the presence of antiviral immune responses and antiretroviral therapy. Annu. Rev. Immunol. *18*, 665–708.

Rafati, H., Parra, M., Hakre, S., Moshkin, Y., Verdin, E., and Mahmoudi, T. (2011). Repressive LTR nucleosome positioning by the BAF complex is required for HIV latency. PLoS Biol. *9*, e1001206.

Ramirez, P.W., Famiglietti, M., Sowrirajan, B., DePaula-Silva, A.B., Rodesch, C., Barker, E., Bosque, A., and Planelles, V. (2014). Downmodulation of CCR7 by HIV-1 Vpu results in impaired migration and chemotactic signaling within $CD4^+$ T cells. Cell Rep. *7*, 2019–2030.

Ramratnam, B., Ribeiro, R., He, T., Chung, C., Simon, V., Vanderhoeven, J., Hurley, A., Zhang, L., Perelson, A.S., Ho, D.D., and Markowitz, M. (2004). Intensification of antiretroviral therapy accelerates the decay of the HIV-1 latent reservoir and decreases, but does not eliminate, ongoing virus replication. J. Acquir. Immune Defic. Syndr. *35*, 33–37.

Razooky, B.S., Pai, A., Aull, K., Rouzine, I.M., and Weinberger, L.S. (2015). A hardwired HIV latency program. Cell *160*, 990–1001.

Rong, L., and Perelson, A.S. (2009). Modeling HIV persistence, the latent reservoir, and viral blips. J. Theor. Biol. *260*, 308–331.

Rueda, C.M., Velilla, P.A., Chougnet, C.A., Montoya, C.J., and Rugeles, M.T. (2012). HIV-induced T-cell activation/exhaustion in rectal mucosa is controlled only partially by antiretroviral treatment. PLoS ONE *7*, e30307.

Sáez-Cirión, A., Bacchus, C., Hocqueloux, L., Avettand-Fenoel, V., Girault, I., Lecuroux, C., Potard, V., Versmisse, P., Melard, A., Prazuck, T., et al.; ANRS VISCONTI Study Group (2013). Post-treatment HIV-1 controllers with a long-term virological remission after the interruption of early initiated antiretroviral therapy ANRS VISCONTI Study. PLoS Pathog. *9*, e1003211.

Søgaard, O.S., Graversen, M.E., Leth, S., Olesen, R., Brinkmann, C.R., Nissen, S.K., Kjaer, A.S., Schleimann, M.H., Denton, P.W., Hey-Cunningham, W.J., et al. (2015). The Depsipeptide Romidepsin Reverses HIV-1 Latency In Vivo. PLoS Pathog. *11*, e1005142.

Toohey, M.G., and Jones, K.A. (1989). In vitro formation of short RNA polymerase II transcripts that terminate within the HIV-1 and HIV-2 promoter-proximal downstream regions. Genes Dev. *3*, 265–282.

Trautmann, L., Labarrière, N., Jotereau, F., Karanikas, V., Gervois, N., Connerotte, T., Coulie, P., and Bonneville, M. (2002). Dominant TCR V alpha usage by virus and tumor-reactive T cells with wide affinity ranges for their specific antigens. Eur. J. Immunol. *32*, 3181–3190.

Trautmann, L., Rimbert, M., Echasserieau, K., Saulquin, X., Neveu, B., Dechanet, J., Cerundolo, V., and Bonneville, M. (2005). Selection of T cell clones expressing high-affinity public TCRs within Human cytomegalovirus-specific CD8 T cell responses. J. Immunol. *175*, 6123–6132.

Van de Griend, R.J., Van Krimpen, B.A., Bol, S.J., Thompson, A., and Bolhuis, R.L. (1984). Rapid expansion of human cytotoxic T cell clones: growth promotion by a heat-labile serum component and by various types of feeder cells. J. Immunol. Methods *66*, 285–298.

Wahl, A., Swanson, M.D., Nochi, T., Olesen, R., Denton, P.W., Chateau, M., and Garcia, J.V. (2012). Human breast milk and antiretrovirals dramatically reduce oral HIV-1 transmission in BLT humanized mice. PLoS Pathog. *8*, e1002732.

Weinberger, A.D., and Weinberger, L.S. (2013). Stochastic fate selection in HIV-infected patients. Cell *155*, 497–499.

Weinberger, L.S., Dar, R.D., and Simpson, M.L. (2008). Transient-mediated fate determination in a transcriptional circuit of HIV. Nat. Genet. *40*, 466–470.

Zhen, A., Rezek, V., Youn, C., Lam, B., Chang, N., Rick, J., Carrillo, M., Martin, H., Kasparian, S., Syed, P., et al. (2017). Targeting type I interferon-mediated activation restores immune function in chronic HIV infection. J. Clin. Invest. *127*, 260–268.

Cell Reports, Volume *21*

Supplemental Information

In Vivo Suppression of HIV Rebound by Didehydro-Cortistatin A, a "Block-and-Lock" Strategy for HIV-1 Treatment

Cari F. Kessing, Christopher C. Nixon, Chuan Li, Perry Tsai, Hiroshi Takata, Guillaume Mousseau, Phong T. Ho, Jenna B. Honeycutt, Mohammad Fallahi, Lydie Trautmann, J. Victor Garcia, and Susana T. Valente

Supplemental Information

Supplemental Figures

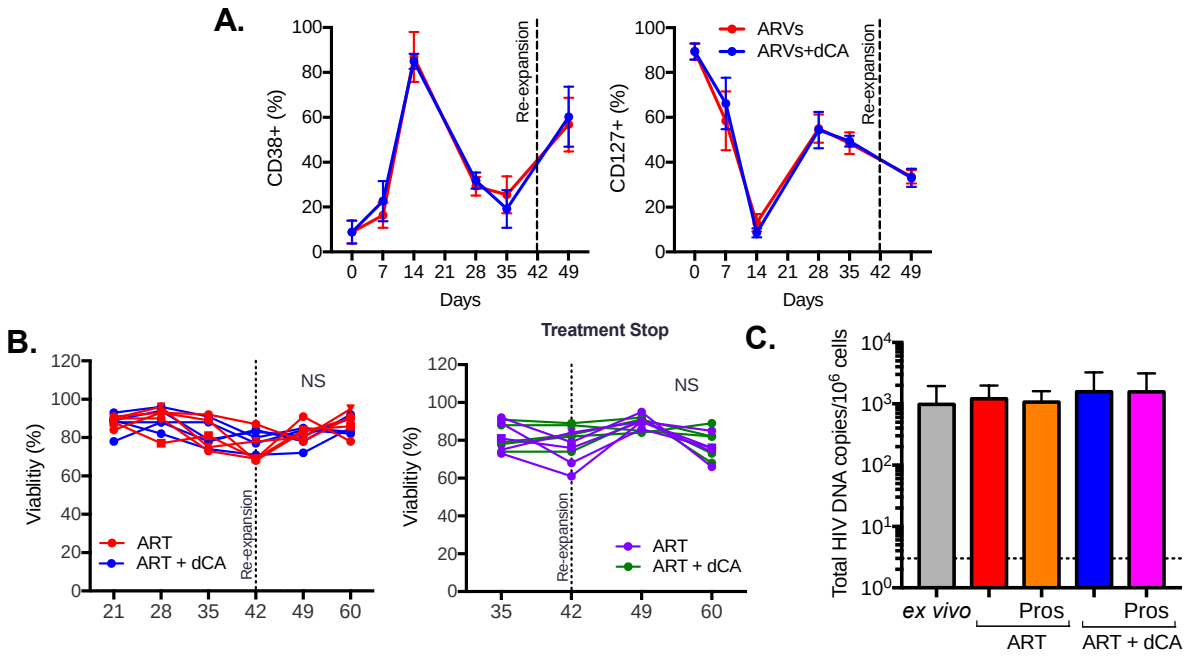

Figure S1. No significant difference in phenotype of cells or viability in treated with dCA compared to ART alone. Related to Figure 1.

(**A**) Primary human $CD4^+$ T cells treated with ART or ART and dCA were analyzed by flow cytometry overtime for activation and quiescence markers (CD38, CD127). There was no change in markers between treatment groups, and as expected, following the expansions, cells became activated. Error bars represent standard deviation.

(**B**) To assess health of cell cultures overtime, cells were stained weekly with trypan blue. No difference in viability of cells between treatment groups or after treatment stop was evident based.

(**C**) Changes in total HIV DNA content occurred due to stimulation, however, total HIV DNA copy numbers did not change between ART and ART + dCA treatment groups. Error bars represent standard deviation.

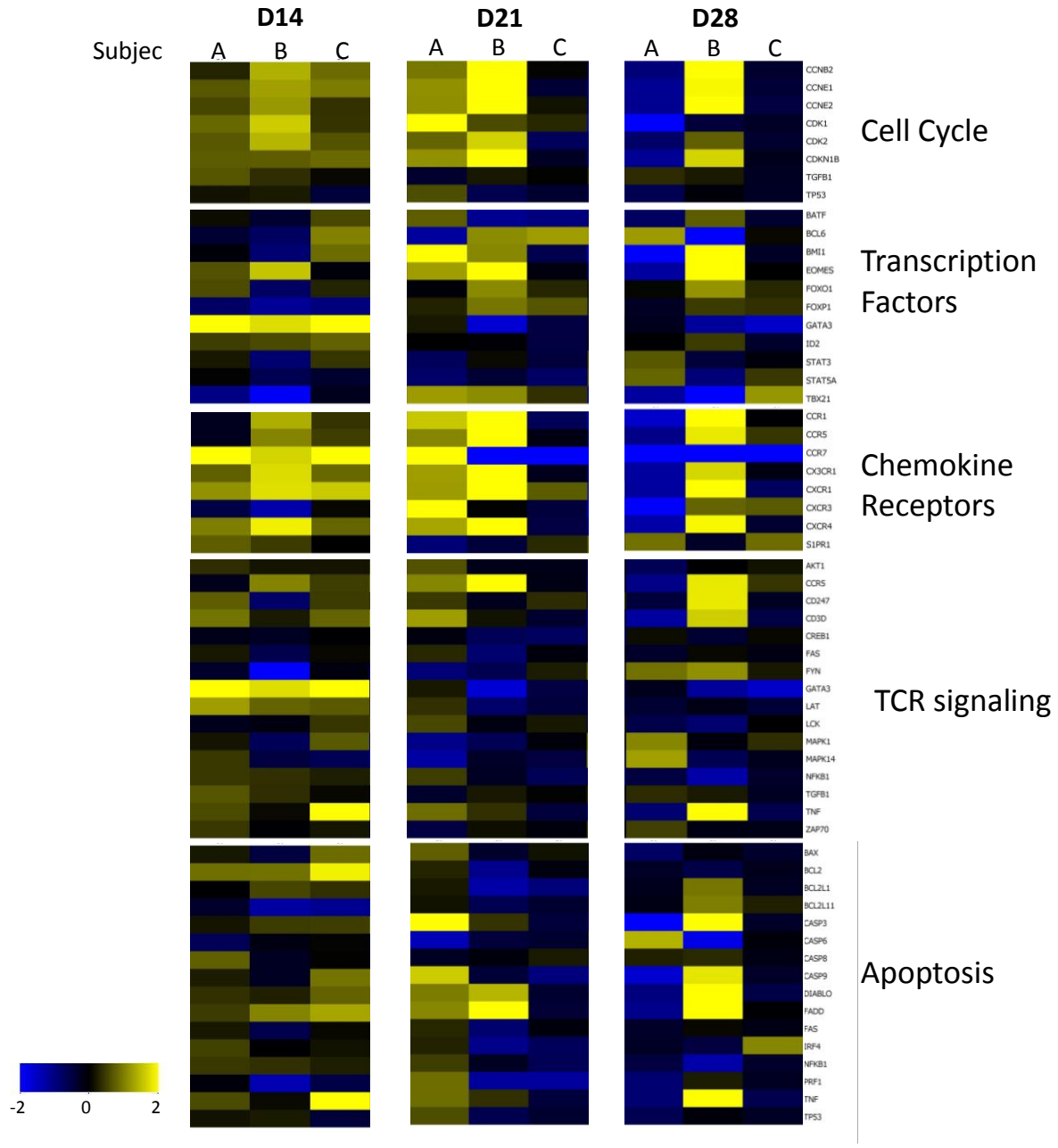

Figure S2. No significant change in gene expression between cells treated with ART or ART and dCA. Related to Figure 1. Targeted gene expression profile of 52 genes by multiplex RT-qPCR involved in cell cycle, transcription factors, chemokine receptors, TCR signaling, and apoptosis of $CD4^+$ T cells treated with ART and ART and dCA over time. Scale represents $\log_2$ fold change in gene expression of 1000 $CD4^+$ T cells in ART and dCA treated compared to cells treated with ART only. RPL13A and IP08 were used as housekeeping genes and fold change was calculated with ARVs treated cells compared to ART and dCA treated cells with all patients combined.

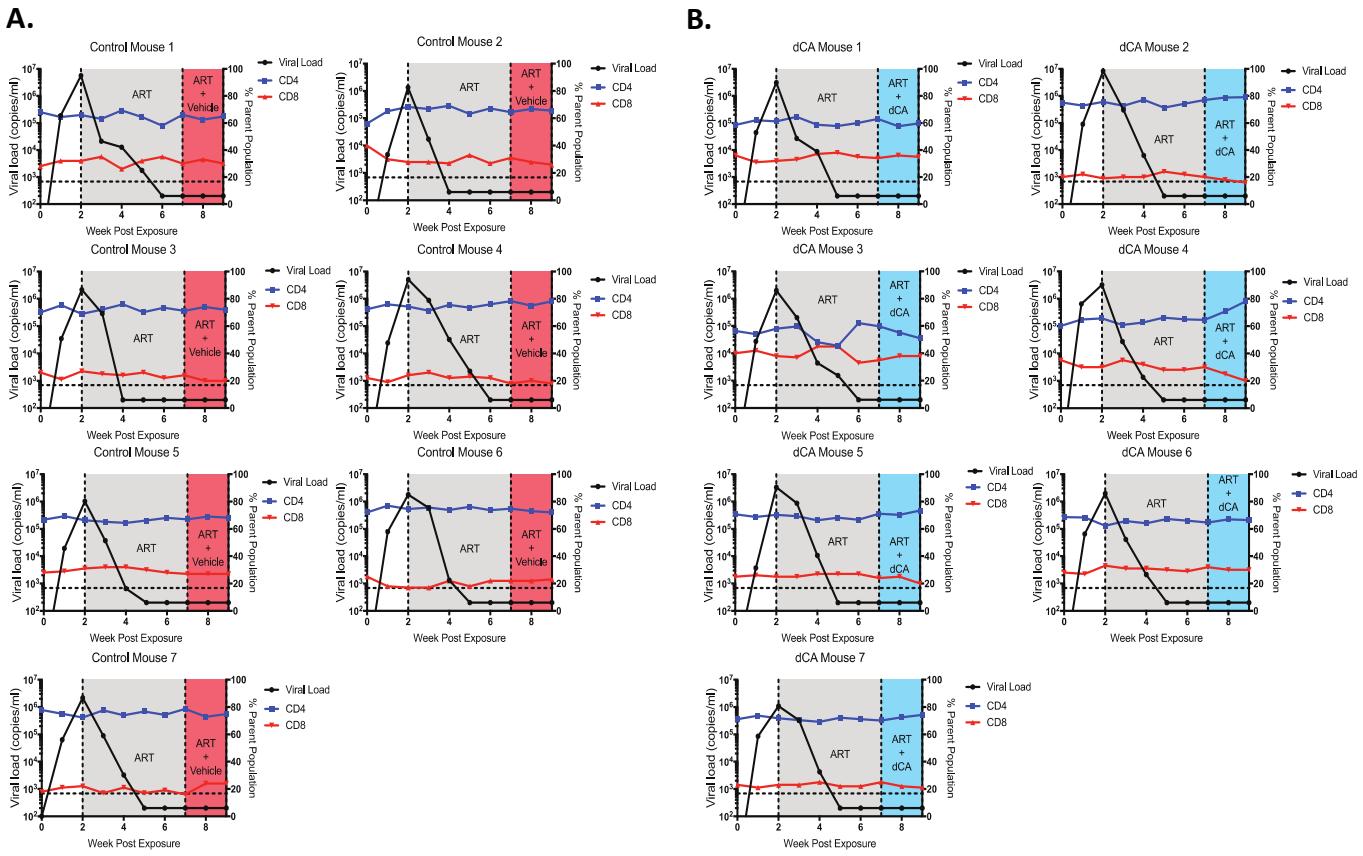

Figure S3. Analysis of the effect of dCA on viral load and T cell levels in peripheral blood. Related to Figure 3.

(**A**) and (**B**) Viral load and T cells levels in mice treated with control vehicle (red, n=7) in addition to ART and mice treated with dCA daily for two weeks (blue, n=7) in addition to ART.

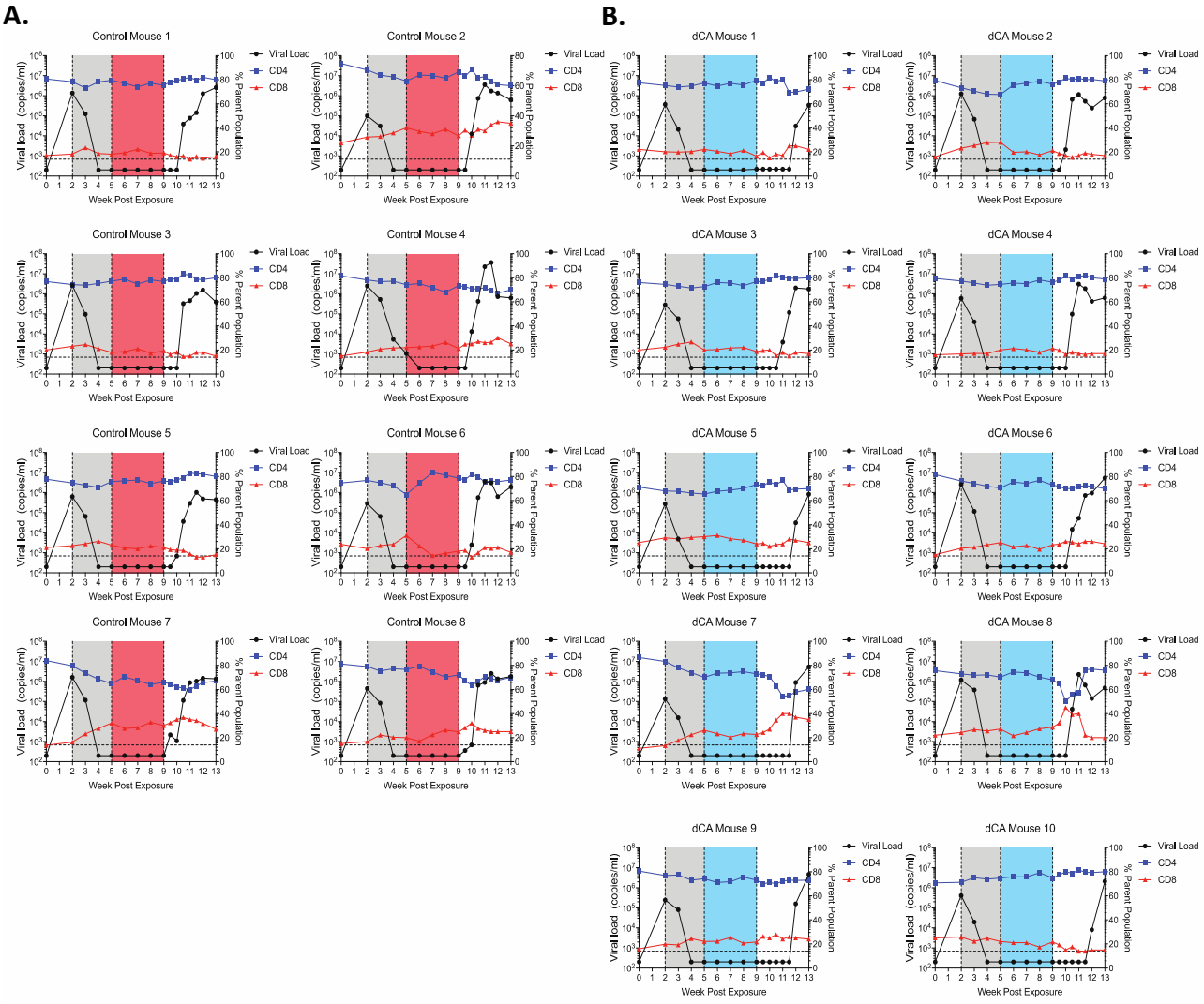

Figure S4. dCA treatment of HIV infected and ART suppressed BLT humanized mice. Related to Figure 4. (**A**) and (**B**) Viral loads in experimental (n=10) and control (n=8) mice were monitored weekly through the course of the experiment. Plots of viral load, human CD4 and CD8 T cell levels in the peripheral blood of individual control (A) and dCA (B) treated mice are shown.

Primer	Sequence
Total HIV and mRNA in primary cells	
CD3OUT5	ACTGACATGGAACAGGGGAAG
CD3OUT3	CCAGCTCTGAAGTAGGGAACATAT
CD3IN5	GGCTATCATTCTTCTTCAAGGT
CD3IN3	CCTCTCTTCAGCCATTTAAGTA
CD3 Taq	LC640AGCAGAGAACAGTTAAGAGCCTCCAT-BBQ
HIV L1	ATGCCACGTAAGCGAAACTCTGGGTCTCTCTDGTTAGAC
HIV R1	CCATCTCTCTCCTTCTAGC
HIV L2	ATGCCACGTAAGCGAAACT
HIV R2	CTGAGGGATCTCTAGTTACC
HIV Taq	LC640-CACTCAAGGCAAGCTTTATTGAGGC-BBQ
Histone ChIP q-PCR	
Nuc-0-F	CCTGATTGGCAGAACTACACAC
Nuc-0-R	TCTACTTGCTCTGGTTCAACTGG
DHS-1-F	TGACAGCCTCCTAGCATTTC
DHS-1-R	CACACCTCCCTGGAAAGTC3
Nuc-1-F	CTGGGAGCTCTCTGGCTAACTA
Nuc-1-R	TTACCAGAGTCACACAACAGACG
Nuc-2-F	GCGACTGGTGAGTACGCCAA
Nuc-2-R	CCCCTGGCCTTAACCGAATTT
GAPDH-F	GGACCTGACCTGCCGTCTAGAA
GAPDH-R	GGTGTCGCTGTTGAAGTCAGAG
Mnase experiments q-PCR	
p1-F	GATCtGTGGATCTACCACAC
p1-R	GCACCATCCAAAGGTCAGTGG
p2-F	CCTGATTGGCAGAACTACACAC
p2-R	TCTACTTGCTCTGGTTCAACTGG
p3-F	CCTTTGGATGGTGCTTCAAGTTAG
p3-R	ATGCTGGCTCATAGGGTGTAAC3
p4-F	GAGCAAGTAGAAGAGGCCAATG
p4-R	GAAATGCTAGGAGGCTGTCA
p5-F	GAGCCAGCATGGGATGG
p5-R	CTCCGGATGCAGCTCTC
p6-F	TGACAGCCTCCTAGCATTTC
p6-R	CACACCTCCCTGGAAAGTC3
p7-F	TACTACAAAGACTGCTGACATCG
p7-R	TCTGAGGGCTCGCCACTC
p8-F	GGGACTTTCCGCTGGGGAC
p8-R	CCCAGTACAGGCAAAAAGCAGC
p9-F	AGTGGCGAGCCCTCAGATG
p9-R	AGCAGTGGGTTCCCTAGTTAGC
p10-F	CCTGTACTGGGTCTCTCTGGTT
p10-R	TTTGAGCACTCAAGGCAAGCTTTA
p11-F	GGTTAGACCAGATCTGAGCCTGG
p11-R	CAACAGACGGGCACACACTACT
p12-F	TCTCTGGCTAACTAGGGAACC
p12-R	AAAGGGTCTGAGGGATCTCTAG
p13-F	CCACTGCTTAAGCCTCAATAAAGCT
p12-R	TCCACACTGACTAAAAGGGTCTGA
p14-F	AGTGTGTGCCCGTCTGTTGTG
p14-R	CTTTCGCTTTCAAGTCCCTGTTCG
p15-F	GTGTGGAAAATCTCTAGCAGTG
p15-R	CTTCAGCAAGCCGAGTCC
p16-F	CGAACAGGGACTTGAAAGCGAAA
p16-R	CGTACTCACCAGTCGCCGC
p17-F	GAGATCTCTCGACGCAGGACT
p17-R	CGCACCCATCTCTCTCCTTCTA
p18-F	GCGACTGGTGAGTACGCCAA
p18-R	CCCCTGGCCTTAACCGAATTT
p19-F	AGAGATGGGTGCGAGAGC
p19-R	GCTCCCTGCTTGCCCATAC

Primer	Sequence
RNPII ChIP q-PCR	
p20-F	GAGCCAGCATGGGATGG
p20-R	CTCCGGATGCAGCTCTC
p21-F	GGGACTTTCCGCTGGGGAC
p21-R	CCCAGTACAGGCAAAAAGCAGC
p22-F	AGTGGCGAGCCCTCAGATG
p22-R	AGCAGTGGGTTCCCTAGTTAGC
p23-F	CTGGGAGCTCTCTGGCTAACTA
p23-R	TTACCAGAGTCACACAACAGACG
p24-F	AGTGTGTGCCCGTCTGTTGTG
p24-R	CTTTCGCTTTCAAGTCCCTGTTCG
p25-F	GTGTGGAAAATCTCTAGCAGTG
p25-R	CTTCAGCAAGCCGAGTCC
p26-F	CGAACAGGGACTTGAAAGCGAAA
p26-R	CGTACTCACCAGTCGCCGC
p27-F	GAGATCTCTCGACGCAGGACT
p27-R	CGCACCCATCTCTCTCCTTCTA
p28-F	GCGACTGGTGAGTACGCCAA
p28-R	CCCCTGGCCTTAACCGAATTT
p29-F	GCAGTCCTCTATTGTGTGCATCAA
p29-R	CCTGTGTCAGCTGCTGCTTG
p30-F	CCATCAATGAGGAAGCTGCAGAA
p30-R	GGTGGATTATGTGTCATCCATCCT
p31-F	TTCTTCAGAGCAGACCAGAGC
p31-R	GCTGCCAAAGAGTGATCTGA
p32-F	CAGAAATACAGAAGCAGGGGCAA
p32-R	GTGTGGGCACCCTTCATTCTT
p33-F	ACTTACGGGGATACTTGGGCAG
p33-R	CTCCATTTCTTGCTCTCCTCTGTC
p34-F	TTGCTCAATGCCACAGCCAT
p34-R	TTTGACCACTTGCCACCCAT
HIV RNA in BLT mice	
HIV gag F	CATGTTTTCAGCATTATCAGAAGGA
HIV gag R	TGCTTGATGTCCCCCCACT
HIV FAM	CCACCCCACAAGATTTAAACACCATGCTAA-Q

Table S1. Related to Experimental Procedures. Sequences of primers and probes used.

Supplemental Experimental Procedures

HIV RNA and DNA collection and extraction. Freshly collected cell culture supernatants were centrifuged for one hour at 30,000 g to pellet HIV particles. Viral RNAs were extracted using the Qiamp viral RNA kit (Qiagen, Hilden, Germany) and quantified using an ultrasensitive semi-nested real time RT-qPCR as previously described (Mousseau et al., 2012; Mousseau et al., 2015). Briefly, extracted viral RNA was reverse transcribed and amplified with the primers and probes (Integrated DNA Technologies, Inc., Coralville, IA). Pre-amplified products were diluted 10-fold and subjected to a nested real time PCR for 40 cycles on the Rotor-Gene Q. In all experiments, serial dilutions of HIV particles (acquired from ACH2 cell culture supernatant, obtained through the NIH AIDS Reagent Program from Dr. Thomas Folks (Clouse et al., 1989; Folks et al., 1989)) in culture medium were processed in parallel of experimental samples to be used as standard. HIV particles used for standard were quantified by digital droplet PCR at University of Miami.
For total HIV DNA, cell pellets were digested at 133 µL/million cells with lysis buffer (10 mM Tris-HCL, 50 nM KCl, 400 µg/ml proteinase K (Invitrogen, Carlsbad, CA), and total HIV DNA content was measured first by PCR amplification with Taq polymerase, 1X Taq Buffer (Invitrogen), $MgCl_2$, dNTPs, HIV and CD3 primers for 12 cycles in triplicate. The second amplification involved a nested PCR using 1:10 of previous amplification product, HIV and CD3 primers, SsoAdvanced Universal Probe Supermix (Biorad, Hercules, CA) using Biorad CFX96 Real-time PCR instrument (Biorad). A standard curve was established using ACH2 cell lysates (ATCC) that contain a single copy of HIV per cell. Primers used are listed in Supplemental Table 1.

***In vitro* phenotypic analysis.** $CD4^+$ T cells were stained for surface markers at 4°C for 20 minutes with the following monoclonal antibodies: αCD4-PE, (Biolegend, San Diego, CA), αCD38-APC, αCD3-A700, αCD45RA-APCH7 (BD Biosciences, San Jose, CA), and αCD127-V450 (Affymetrix eBioscience, Waltham, MA). Live/dead stain was used to exclude dead cells and quantify viability. Cells were then fixed with 2% formaldehyde in PBS. Stained $CD4^+$ T cells were run on an LSRII flow cytometer using DiVA software (BD Biosciences) and analyzed with FlowJo (Treestar, Ashland, OR).

Gene expression analysis. $CD4^+$ T cells were sorted into 96-well plates at 1000 cells/well to perform the Fluidigm's Biomark Assay. Assays (Primers and Probes) were designed using the Roche Universal Probe Library Assay Design Center (www.universalprobelibrary.com) and were designed to detect multiple transcripts (Roche). $CD4^+$ T cells were sorted directly into PCR plates containing PCR 5X buffer mix and immediately snap frozen. RNA was reverse transcribed and amplified in a single-step RT-STA (Specific Template Amplification) using a pool of all the primer sets and with the Superscript III Platinum One-Step qRT-PCR Kit (without ROX) (Life Technologies, Waltham, MA). The PCR was carried out for 18 cycles at 95°C for 15 seconds and 60°C for four minutes. High-throughput qPCR on the pre-amplified samples was performed on a 96.96 BioMark™ Dynamic Array (Fluidigm, San Francisco, CA) for 40 cycles (15 s at 95°C, 5 s at 70°C, 60 s at 60°C). The same primer set used in the RT-PCR was used for the probe-based qPCR. Threshold cycle (CT) values were calculated by the Real-Time PCR Analysis Software (Fluidigm). RPL13A and IPO8 were used as housekeeping genes and fold change was calculated between ART treated cells compared to ART and dCA treated cells with all patients combined. The lowest expression Ct value for each gene was used as a calibrator to calculate relative mRNA expression levels. GeneSpring GX 12.1 (www.agilent.com) was used to analyze the raw Cq dataset. The raw Cq tab-delimited file was imported into GeneSpring. The normalization method was set to "Quantile" and the significance analysis parameters were set as follows: p-value computation: Asymptotic, p-value correction: Benjamini-Hochberg, p-value cut-off: 0.05, fold change cut-off: 2. The heatmaps were generated using GeneSpring based on minus delta-delta Cq values.

Chromatin immunoprecipitation assay. The chromatin immuno-precipitation (ChIP) assay was performed as previously described with some modifications (Mousseau et al., 2012; Mousseau et al., 2015). HIV latently infected OM10.1 cells were maintained in RPMI 1640 medium containing 10% fetal bovine serum and PSG (100 IU/ml penicillin, 100 µg/ml streptomycin, 2 mM L-glutamine), and treated with ART (200 nM Lamivudine, 200 nM Raltegravir and 100 nM Efavirenz) or ART plus 100 nM dCA respectively. Cells were stimulated with SAHA for 8 h and crosslinked with 1% formaldehyde. Pellets of $1x10^7$ cells were sonicated 18 times for 10-s bursts on ice to generate sheared chromatin of 200 to 400 nucleotides. The equivalent of $5x10^6$ cells were used for each IP assay with anti-RNAP II (05-623; Millipore), normal mouse IgG (NI03; Millipore), anti-H3 (07-690; Millipore), or normal rabbit IgG (NB810569101; Fisher Scientific). The equivalent of 1% chromatin was saved as an input control. Immunoprecipitated DNA was eluted with elution buffer (0.1 M NaHCO3, 1% SDS). DNA samples were reverse cross-linked for 4h at 65°C in the presence of 200 mM NaCl, and then digested with proteinase K (BP1700100; Fisher Scientific) in the presence of EDTA (10 mM) and Tris-HCl (40 mM, pH 6.5) at 45°C for 1h. After 30 min of RNase A (MRNA092; Epicentre Technologies) treatment at 37°C, the DNA was purified by using PCR Clean kit (Qiagen). Primers used are listed in Supplemental Table 1. Input (1%) was used to standardize the values obtained.

The relative proportions of coimmunoprecipitated DNA fragments were determined on the basis of the threshold cycle (C_T) for each qPCR product. The data sets were normalized to input values {percent input=2[C_T(input)-C_T(IP)] ×100}. The average value of the IgG background for each primer was subtracted from the raw data.

High resolution nucleosomal mapping. Nucleosome position were monitored based on the method of Jadlowsky and Rafati with some modifications (Jadlowsky et al., 2014; Rafati et al., 2011). Briefly, cells were cross-linked similarly to ChIP protocol above, then washed with buffer B (0.25% Triton-X 100, 1 mM EDTA, 0.5 mM EGTA, 20 mM Herpes, pH 7.6), buffer C (150 mM NaCl, 1 mM EDTA, 0.5 mM EGTA, 20 mM Herpes, pH 7.6). After one wash in cold PBS, 1.5×10^7 cross-linked cells were re-suspended in 1 mL hypotonic buffer A (300 mM sucrose, 2 mM Mg Acetate, 3 mM $CaCl_2$, 10 mM Tris-HCl pH 8.0, 0.1% Triton X-100, 0.5 mM DTT), incubated on ice for 5 min, and dounced 20 times with 2 mL dounce homogenizer (tight pestle, Wheaton). Nuclei were collected by centrifuging at 4°C for 5 min at 720×g. Pellets were re-suspended in 1 mL buffer D (25% glycerol, 5 mM Mg acetate, 50 mM Tris-HCl pH 8.0, 0.1 mM EDTA, 5 mM DTT) at 1.5×10^7 nuclei/mL. Chromatin was collected by centrifuging at 4°C for 5 min at 720×g. The pellets were re-suspended in 1 mL buffer MN (60 mM KCl, 15 mM NaCl, 15 mM Tris-HCl pH 7.4, 0.5 mM DTT, 0.25 mM sucrose, 1.0 mM $CaCl_2$) at 2.5×10^7 nuclei/mL. The equivalent of 2.5×10^6 nuclei were used per digestion reaction. Micrococcal nuclease (50645000; Fisher Scientific), diluted in buffer MN, was added so that 25 (Digested) and 0.25 (Undigested) total units were used per 100 µL reaction and digested for 30 min at room temperature. Reactions were stopped with EDTA and SDS at 12.5 mM and 0.5% respectively final concentrations. After 4 hrs of proteinase K digestion at 37°C, each sample was de-crosslinked overnight at 65°C in presence of 200 mM NaCl. The products were digested with RNase for 30 min and purified with PCR Clean kit (Qiagen). Eluted products were run on a 1% agarose gel to confirm MNase digestion. After measuring the concentration, the DNA samples were diluted to the same concentration (5 ng/µl) and used for real-time qPCR analysis (Bio-rad, CFX96^{TM} Real-Time System) using primers in Supplemental Table 1. The fold difference was calculated using delta C_T method between digested and undigested samples.

Exposure of BLT humanized mice to HIV, plasma viral load analysis and tissue RNA analysis. Exposure of BLT mice to HIV-1_{JRCSF} was conducted via tail vein injection with $3x10^4$ tissue culture infectious units (TCIU) of virus. Plasma viral load in peripheral blood of infected mice was monitored longitudinally by quantitative real-time PCR using TaqMan® RNA to-C_TTM 1-step kit (Applied Biosystems, Foster City, CA) as described (Wahl et al., 2012). RNA from tissue was extracted using QIAamp viral RNA columns (Qiagen) according to the manufacturer's protocol including an optional treatment with RNase-free DNase and analyzed using one-step reverse transcriptase real-time PCR [ABI custom TaqMan Assays-by-Design] (Krisko et al., 2013). The sequences of the forward and reverse primers and the TaqMan® probe for PCR amplification and detection of HIV gag RNA are listed in Supplemental Table 1. For viral load analysis, 40 µl of plasma was collected and analyzed with a sensitivity of 687 copies/mL. Known quantities of HIV gag RNA standards were run in parallel, creating a standard curve for HIV gag and sample RNA was quantified by extrapolation from the standard curve. For lymphoid tissue RNA analysis nucleic acid was extracted using QIAamp viral RNA columns (Qiagen) according to the manufacture's protocol including an optional treatment with RNase-free DNase and analyzed using one-step reverse transcriptase real-time PCR [ABI custom TaqMan Assays-by-Design] (Krisko et al., 2013). HIV RNA levels were normalized by the number of $CD4^+$ T cells. For brain tissue samples where no flow cytometry data was available due to the small sample size, levels of HIV gag RNA were normalized to levels of human tata binding protein RNA using the ddCT method (Livak and Schmittgen, 2001). All samples were run and analyzed on an ABI 7500 Fast Real Time PCR System (Applied Biosystems, Foster City, CA).

Antiretroviral therapy. ART to treat HIV infection was administered to BLT mice via 1/2″ pellets of irradiated Teklad chow consisting of emtricitabine (1500 mg/kg), tenofovir disoproxil fumarate (1560 mg/kg), and raltegravir (600 mg/kg) (Research Diets, New Brunswick, NJ).

***In vivo* phenotypic analysis.** Antibodies used for the *in vivo* study include: anti-CD45 APC (clone HI30; BD Pharmingen, San Jose, CA), anti-CD3 FITC (clone HIT3a; BD Pharmingen), anti-CD4 PE (clone RPA-T4; BD Pharmingen), and anti-CD8 PerCP (clone SK1; BD Biosciences). All samples were acquired on a FACSCanto (BD Biosciences) flow cytometer and post-acquisition analysis was performed with FlowJo software (FlowJo LLC). Immunophenotyping was performed on blood samples collected longitudinally and on mononuclear cells isolated from tissues at harvest. Whole peripheral blood from humanized mice was analyzed according to the BD Biosciences Lyse/Wash protocol (Cat. No. 349202). Briefly, following antibody labeling of whole blood, red blood cells were lysed, and the remaining cells were washed, fixed and the sample was analyzed by flow cytometry. Flow cytometric gating for expression of lineage specific antigens on human leukocytes was performed as follows: (step 1) forward and side scatter properties were utilized to set a live cell gate; (step 2) live cells were then analyzed for

expression of the human pan- leukocyte marker CD45; (step 3) human leukocytes were then analyzed for hCD3 and (step 4) T cells or thymocytes were analyzed for hCD4 and hCD8 expression.

dCA administration to BLT mice. dCA was initially dissolved in DMSO (Sigma-Aldrich) and then diluted with sterile saline and filtered through a 0.22-micron nylon syringe filter (Fisher Scientific). The drug was administered by intraperitoneal injection daily at a dose of 0.5 mg/kg.

Statistical analysis. P-values for *in vitro* experiments were calculated using one-way ANOVA and Kruskal-Wallis with post-hoc Dunn multiple comparison analysis or paired T-test with 95% confidence intervals using the Prism 7 for Macintosh (GraphPad software, La Jolla, CA). All *in vivo* statistical analyses were also performed in Prism 7. A two-tailed Mann-Whitney U test was used to compare levels of viral RNA in dCA treated mice with control vehicle treated mice.

Supplemental References

Clouse, K.A., Powell, D., Washington, I., Poli, G., Strebel, K., Farrar, W., Barstad, P., Kovacs, J., Fauci, A.S., and Folks, T.M. (1989). Monokine regulation of human immunodeficiency virus-1 expression in a chronically infected human T cell clone. J Immunol *142*, 431-438.

Folks, T.M., Clouse, K.A., Justement, J., Rabson, A., Duh, E., Kehrl, J.H., and Fauci, A.S. (1989). Tumor necrosis factor alpha induces expression of human immunodeficiency virus in a chronically infected T-cell clone. Proc Natl Acad Sci U S A *86*, 2365-2368.

Jadlowsky, J.K., Wong, J.Y., Graham, A.C., Dobrowolski, C., Devor, R.L., Adams, M.D., Fujinaga, K., and Karn, J. (2014). Negative elongation factor is required for the maintenance of proviral latency but does not induce promoter-proximal pausing of RNA polymerase II on the HIV long terminal repeat. Mol Cell Biol *34*, 1911-1928.

Krisko, J.F., Martinez-Torres, F., Foster, J.L., and Garcia, J.V. (2013). HIV restriction by APOBEC3 in humanized mice. PLoS Pathog *9*, e1003242.

Livak, K.J., and Schmittgen, T.D. (2001). Analysis of relative gene expression data using real-time quantitative PCR and the 2(-Delta Delta C(T)) Method. Methods *25*, 402-408.

Mousseau, G., Clementz, M.A., Bakeman, W.N., Nagarsheth, N., Cameron, M., Shi, J., Baran, P., Fromentin, R., Chomont, N., and Valente, S.T. (2012). An analog of the natural steroidal alkaloid cortistatin A potently suppresses Tat-dependent HIV transcription. Cell Host Microbe *12*, 97-108.

Mousseau, G., Kessing, C.F., Fromentin, R., Trautmann, L., Chomont, N., and Valente, S.T. (2015). The Tat Inhibitor Didehydro-Cortistatin A Prevents HIV-1 Reactivation from Latency. MBio *6*, e00465.

Rafati, H., Parra, M., Hakre, S., Moshkin, Y., Verdin, E., and Mahmoudi, T. (2011). Repressive LTR nucleosome positioning by the BAF complex is required for HIV latency. PLoS Biol *9*, e1001206.

Wahl, A., Swanson, M.D., Nochi, T., Olesen, R., Denton, P.W., Chateau, M., and Garcia, J.V. (2012). Human breast milk and antiretrovirals dramatically reduce oral HIV-1 transmission in BLT humanized mice. PLoS Pathog *8*, e1002732.